Study on Dynamic Adsorption and Desorption Processes of Hexavalent Chromium Using Aerobic Granular Sludge System

July 2020

TIAN Caixing

Study on Dynamic Adsorption and Desorption Processes of Hexavalent Chromium Using Aerobic Granular Sludge System

A Dissertation Submitted to

the Graduate School of Life and Environmental Sciences,

the University of Tsukuba

in Partial Fulfillment of the Requirements

for the Degree of Doctor of Philosophy in Environmental Studies

(Doctoral Program in Sustainable Environmental Studies)

TIAN Caixing

Abstract

With the rapid growth of global population and the continuously industrial expansion, the water pollution caused by heavy metals has become a serious environmental issue. Chromium (Cr) contamination is one of them, which has a wide range of industrial sources and high toxicity. As a common valence state, hexavalent chromium (Cr (VI)) is considered to be highly lethal to most organisms due to its high water solubility, high toxicity, carcinogenicity and mutagenicity. Various technologies have been trialed to treat the Cr-containing wastewater, including physical, chemical and biological methods. Among them, biosorption has gradually attracted more researchers' attention because of its simple operation, low cost and less secondary pollution. As an emerging technology and efficient biomaterial, aerobic granular sludge (AGS) has been attempted for Cr (VI) adsorption from wastewater due to its high concentration of biomass retention and dense structure. However, up to now, few studies focused on the bioactivity and sustainability of AGS during and after Cr (VI) adsorption. Considering the difficulty in Cr-loaded AGS disposal and the long time requirement for AGS formation, this study for the first time explored dynamic adsorption/desorption processes on AGS in order to realize the reuse and recycling of AGS, and removal and recovery of Cr from wastewater.

Firstly, the effects of Cr (VI) desorption on AGS bioactivity and stability were investigated in batch tests. Results show that among the five desorbents tested, sodium carbonate (Na_2CO_3) was found to be the most effective one for the desorption of Cr (VI) from Cr-loaded AGS. When 1 M Na_2CO_3 was used, the desorption efficiency of Cr (VI) was 33.65 ± 0.76% in 180 min, which increased with the increase in Na_2CO_3 concentration and contact time. In comparison to the pseudo-first-order kinetic model, the desorption data showed a better fit to the pseudo-second-order kinetic one (R^2 = 0.985-0.995). Specific oxygen uptake rate (SOUR) was detected to decrease from the initial 22.38 ± 1.37 mg-O_2/g-VSS·h to 5.55 ± 1.42 mg-O_2/g-VSS·h when the desorption was processed in 1M Na_2CO_3 for 60 min, with the integrity coefficient increased from 5.52% to 25.63%. During the desorption process, the loss of cations such as Ca^{2+}, Mg^{2+} and K^+ in the AGS mainly came from EPS, especially tightly bound part (TB-EPS), which is likely the main reason for the decline of granular bioactivity and stability. In addition, proteins rather than polysaccharides in extracellular polymeric substances (EPS) were found to be more sensitive to the increasing Na_2CO_3 concentration during the desorption process.

Secondly, the effects of dynamic adsorption/desorption on AGS were studied in sequencing batch reactors (SBRs). This dynamic process shows some decrement effect

(about 11%) on Cr (VI) removal, with a cumulative Cr (VI) removal of 1.87 or 2.11 mg, respectively on day 35 with or without dynamic adsorption/desorption process. Under no dynamic adsorption/desorption (control) condition, the granule settleability was better, while reflected a cumulative inhibitory effect on nitrification. On the other hand, the test reactor under dynamic adsorption/desorption demonstrated mitigated inhibition effect of Cr (VI) on NH_4^+-N removal after operation for 13 days. Results from three different AGS desorbed biomass proportion (25%, 50%, 75%) and two desorption frequencies (1 time/d, 1 time/2d) show that the biomass desorption ratio has limited effect on the cumulative Cr (VI) adsorption amount, but greatly impacted the cumulative desorbed Cr (VI) amount with maximum value obtained in the reactor with 75% biomass desorption ratio. In addition, desorption frequency at 1 time/2d was conducive to the cumulative Cr (VI) adsorption amount, while 1 time/d achieved a higher cumulative desorbed Cr (VI) amount. After 13 days' operation, all the test reactors to some extent demonstrated similar mitigation effects on the inhibition of bioactivity and NH_4^+-N removal caused by Cr (VI), which is more obviously at 1 time/d in the reactor with 50% biomass desorption ratio during days 25-30.

Lastly, the effects of different organic loading rates (OLRs) on the removal and recovery of Cr (VI) in addition to the changes of physicochemical characteristics of AGS were investigated under dynamic adsorption/desorption condition. The AGS system operated at a higher OLR (2 kg COD/m^3·day) obtained Cr (VI) adsorption amount of 2.15 mg and desorption amount of 0.46 mg Cr (VI), respectively, which were apparently higher than those of other two reactors at lower OLRs. During the adsorption/desorption, all the indices relating to AGS properties and bioactivities worsened, including SOUR, integrity coefficient, biomass centration, settling velocity, size and morphology, especially at low OLRs. A higher OLR (2 kg COD/m^3·day tested in this study) was found to be beneficial for the maintenance of AGS stability during Cr-containing wastewater treatment by using dynamic adsorption/desorption AGS system.

Results from this study imply that dynamic adsorption/desorption process could be promising for continuous Cr (VI) removal by AGS and the recycling of AGS. This work can also provide experimental evidence and theoretical support for the application of dynamic adsorption/desorption process in the treatment of other heavy metal-containing wastewater by using the novel AGS biotechnology.

Keywords: Aerobic granular sludge (AGS); Cr (VI); Dynamic adsorption/desorption; Organic loading; Wastewater treatment

Contents

List of tables

List of figures

Acronyms and abbreviations

AGS	Aerobic granular sludge
AS	Activated sludge
BSA	Bovine serum albumin
Ca^{2+}	Calcium ion
Cr	Chromium
Cr (II)	Divalent chromium
Cr (III)	Trivalent chromium
Cr (VI)	Hexavalent chromium
DO	Dissolved oxygen
EDX	Energy Dispersive X-ray
EPS	Extracellular polymeric substances
F/M	Food to microorganism ratio
FTIR	Fourier Transform Infrared
H/D	Ratio of height to diameter
HMs	Heavy metals
HRT	Hydraulic retention time
Ksp	Solubility product
LB-PN	Loosely bound PN
ML(V)SS	Mixed liquor (volatile) suspended solids
N	Nitrogen
Na_2CO_3	Sodium carbonate
$NaHCO_3$	Sodium bicarbonate
Na_2HPO_4	Disodium phosphate
Na_2SO_4	Sodium sulfate
OLR	Organic loading rate
ORP	Oxidation-reduction potential
P	Phosphorus
PBS	Phosphate buffer saline
PN	Proteins
PS	Polysaccharides
SBR	Sequencing batch reactor
SD	Standard deviation
SND	Simultaneous nitrification and denitrification
SOUR	Specific oxygen uptake rate
SRT	Sludge retention time
SVI_5	Sludge volume index after 5 min sedimentation
SVI_{30}	Sludge volume index after 30 min sedimentation
TB-EPS	Tightly bound-EPS

TB-PN	Tightly bound PN
USEPA	United States Environmental Protection Agency
WWTP	Wastewater treatment plant
ZVI	Zerovalent iron

Chapter 1 Introduction

The continuous industrialization and rapid population growth worldwide have led to a significant increase in energy consumption, solid waste production and wastewater discharge. Among them, the problem of wastewater discharge is becoming more and more serious, leading to the deterioration of the environment and seriously affecting the safety of food chain and human health. With the improvement of people's awareness of environmental protection, the problem of water environment pollution has become one of the focuses of environmental protection and governance.

This chapter addresses the water environment issues, especially the pollution caused by chromium-containing wastewater and existing treatment methods. The basic knowledge and application of the new aerobic granular sludge (AGS) technology are also introduced, with the research theme and purpose being arrived at last.

1.1 Water environment pollution

Water pollution is a worldwide problem and it has great potential to affect human health. In fact, the impact of water pollution is considered to be the main cause of human death worldwide, and water pollution widely affects natural body of water, making it a global concern (Khan and Ghouri, 2011). It was reported that one-sixth and more than one-third of the world’s population lack access to safe water and lack basic sanitation facilities, respectively (Khan and Ghouri, 2011). The main sources of water pollution come from domestic sewage, industrial discharge and agricultural activities, including fertilization and spraying of pesticides. In many areas or regions, a large amount of domestic sewage containing toxic substances, solid waste, plastic garbage and bacterial pollutants is discharged into natural water bodies without treatment, which has triggered water pollution. Different industrial wastewater discharged into natural water bodies without proper treatment is another major cause of water pollution (Kamble, 2014). Harmful substances emitted by industry are the cause of surface water and groundwater pollution. It was reported that only 60% of the fertilizer is used in the soil, and the remaining chemicals are immersed in the soil which will further contaminate the water environment. Excessive nutrients such as phosphorus and nitrogen runoff lead to eutrophication and deteriorate water quality. Pesticides containing chemical substances will directly pollute the water environment and affect water quality (Mehtab et al., 2017).

1.2 Heavy metal pollution problems in water

The global water pollution situation is becoming more and more serious. With the continuous industrialization, the pollution caused by industrial wastewater is becoming increasingly prominent, especially heavy metal pollution. Human activities from industry, mining, agriculture sectors may release heavy metals into the environment (Cao et al., 2017). Various sources of different heavy metals are shown in Table 1-1 (Paul, 2017). Because of its non-biodegradability and bioaccumulation through the food chain, heavy metals, a kind of inorganic pollutants, have a variety of negative effects on organisms.

Some heavy metals, such as Cr, Cd and Pb, without any biological functions, are toxic elements that are not easily biodegradable in living organisms. Moreover, they usually cause adverse effects on animals and humans with its accumulation exceeding certain limits (Pandey and Sharma, 2014; Singare, 2012). For example, Pb is known to be toxic to nerves, especially for children, due to its ability to compete with calcium (Ca^{2+}) for nerve function (Lidsky and Schneider, 2003). It is known that the accumulation and reduction of Cr (VI) in cells can cause DNA damage. According to a previous report, Cd has a significant inhibitory effect on microbial activity, showing a downward change in respiratory intensity, urease and catalase activities with the increase of Cd concentration (Shi and Ma, 2017).

1.3. State of the art of chromium-containing wastewater treatment

1.3.1 Hazardousness and source of chromium-containing wastewater

Chromium (Cr) has important applications in industries as a heavy metal, while it also poses a significant threat to organisms due to its high toxicity. Cr is a transitional heavy metal element with oxidation state ranging from Cr (II) to Cr (VI). Among them, hexavalent chromium (Cr (VI)) and trivalent chromium (Cr (III)) as the most common and stable forms have different physiochemical properties and different ways to affect living organisms (Dhal et al., 2013). Cr (VI) with the strongest oxidation potential, the most toxic, and strong water solubility, usually exists in the form of chromate or dichromate ions (Sultana et al., 2014). In contrast, Cr (III) with poor mobility and easily formed precipitates usually can complex with organic matter in the form of chromium oxide, hydroxide or sulfate in the soil and aquatic environment (Emamverdian et al., 2015). Cr (VI) and Cr (III) can be converted to each other under certain conditions. Various environmental conditions including pH, dissolved oxygen (DO), redox potential, some organic/inorganic substances and complexation factors can affect the ratio of Cr

(VI)/Cr (III) in the water (Sinha et al., 2018).

Cr (VI) has been identified by the US Environmental Protection Agency (USEPA) as one of the 17 chemical substances that pose the greatest threat to humans (Marsh and McInerney, 2001). Cr (VI) is the most mobile anion form and has the highest bioavailability in an aqueous environment. Cr (VI) is not only highly toxic to various forms of bacteria, but also mutagenic to bacteria. Besides, Cr (VI) can also causes carcinogenic and mutagenic effects on humans and animals, causing decreased reproductive health and birth defects (Kanojia et al., 1998; Losi et al., 1994). Cr (VI) with a high positive oxidation-reduction potential (ORP) can penetrate the cell membrane to destroy cells and cellular molecular components, resulting in membrane destruction, protein degradation, DNA changes, and induction of mutations in living organisms (Oliveira, 2012; Shanker and Venkateswarlu, 2011). As known, Cr (VI) can cause lung cancer, impair liver and kidney function and may cause nausea, upper abdominal pain, allergic reactions, vomiting, gastric bleeding and ulcers (McCarroll et al., 2010; Sinha et al., 2018).

Since it is easy to spread through the aquatic system and groundwater beyond the initial pollution site, Cr (VI) as the most common form of existence is a harmful pollutant, which mainly comes from human activities such as leather tanning, mining, Cr plating, steel and automobile manufacturing, cement, metal processing, cleaning agents, pigment production, wood processing, organic synthesis and dyes (Alloway, 2013; Kamaludeen et al., 2003). Among them, stainless steel and alloy preparation consumes 60-70% of the world's total output. The use rate of Cr (VI) exceeds 15% in some chemical industrial processes including pigment production, electroplating, leather tanning, etc. (Saha et al., 2011). Cr as a tanning agent is used in about 80-90% of the leather industry. The wastewater from these tannery plants contains approximately 40% Cr in Cr (VI) with Cr (III) salts being the dominant (Sundaramoorthy et al., 2010).

1.3.2 Technologies applied to cope with chromium-containing wastewater

As Cr (VI)-containing wastewater released by human activities can cause environmental pollution and serious health issues, various physical/chemical methods, including adsorption, reduction, ion exchange, chemical precipitation, electrodialysis and reverse osmosis have been applied to treat Cr (VI)-containing wastewater (Jobby et al., 2018). Most of these methods are costly and suffer from disadvantages such as incomplete removal, consumption of large amounts of chemicals and energy, and at the same time contaminate groundwater due to the generation/disposal of toxic sludge/secondary waste.

These methods are not economically feasible at low concentrations (1-100 mg/L), which becomes one of the main limitations of some treatment methods (Addour et al., 1999; Cossich et al., 2004). Bioremediation seems to be a potentially feasible method to tackle the dilemma of low heavy metal concentration in wastewater. Therefore, heavy metals removal and recovery via metal-microbe interaction has become one of the research hotspots (Rahman and Singh, 2020). As reported, bioremediation technology is more effective for metals removal from soluble and particulate forms, especially from dilute solutions, thus microbial-based removal techniques may become the promising options for coping with low Cr concentration wastewater in comparison to the traditional metal removal/recycling technologies (Ozdemir et al., 2004; Chaturvedi et al., 2015).

1.4 Potentials of aerobic granular sludge for Cr removal and recovery

Aerobic granular sludge (AGS) is one of the most promising and versatile biological wastewater treatment processes, and is attracting increasing interest from researchers working in the field of wastewater treatment. Compared to the traditional activated sludge process, the performance of AGS is superior in many aspects, due to its unique physical and chemical properties, such as higher biomass density, stronger agglomeration structure, good settleability, high biomass retention and strong resistance to various loads (Liu et al., 2009).

1.4.1 AGS properties and indicators

(1) Settling velocity and SVI_5

The higher settling velocity of AGS means efficient solid-liquid separation, which is a key parameter in wastewater treatment. The settling of AGS (25 - 70 m/h) is much faster than that of activated sludge (AS) (7 - 10 m/h) (Liu et al., 2003b; Qin et al., 2004). The higher the settling velocity means the more retention of biomass in the reactor, and the stronger the system's capability to degrade organic matters (Adav et al., 2008).

AGS with a large granular size (> 0.2 mm) have a clear sphere and density and can quickly sink through sedimentation, which is conducive to the realization of rapid separation of sludge from treated water (Nancharaiah and Kiran Kumar Reddy, 2018). In addition, it is recommended to use sludge volume index after 5 min sedimentation (SVI_5) to indicate AGS excellent settleability. The ratios of SVI_5 to SVI_{30} within 10% can signal the formation of sludge aggregates (Liu et al., 2010).

(2) Extracellular polymeric substances (EPS) and functions

EPS, an important part of AGS, play an important role in microbial aggregation,

granular formation and maintaining stability. It is reported that EPS extracted from AGS are stickier than the extract from AS (Seviour et al., 2010).

Based on the fact that microorganisms and polysaccharides (PS) are mainly distributed on the outer edges of AGS, while the center has no cells and is mainly composed of proteins (PN), it is predicted that the core of the central protein may play an important role in the formation and stability of AGS (McSwain et al., 2005). The results from Energy Dispersive X-ray (EDX) and Fourier Transform Infrared (FTIR) spectra show that the interaction between molecules contributes to the stability of EPS. The β-D-glucopyranose polysaccharide formed by the internal particles ensures that the AGS of 700 μm size are small and relatively stable (Hamiruddin et al., 2019).

(3) Diverse microbial communities

The AGS structure and the cultivated medium composition play an important role in the microbial diversity of AGS. *Proteobacteria* show superiority in microbial diversity in both phenol-fed AGS and wastewater treatment plants (Jiang et al., 2004; Snaidr et al., 1997; Whiteley and Bailey, 2000). A variety of bacteria have been identified in AGS cultured under various operating conditions, including phosphorus/glycogen accumulation bacteria, nitrifying bacteria, heterotrophic bacteria, denitrifying bacteria (Adav et al., 2008).

1.4.2 Factors affecting cultivation of AGS

Many operating parameters can affect the granulation process, such as seed sludge, feed composition, food to microbe (F/M) ratio or organic loading rate (OLR), metal ions, hydraulic retention time (HRT) and solids retention time (SRT), settling time, and hydrodynamic shear force, configuration of reactor, etc.

(1) Seed sludge

In most studies on AGS, activated sludge (AS) is usually used as the seed sludge for the cultivation of AGS. The bacterial community in AS plays an important role in the formation of AGS (Zita and Hermansson, 1997). Hydrophobic bacteria in seed sludge can promote the granulation process and enhance the settlement performance of AGS (Wilén et al., 2008). Anuar et al. (2020) observed the obvious differences in the microbial community between the seed sludge and AGS during the granulation process in sequencing batch reactor (SBR), in which *Pseudomonas fluorescens* was the most abundant species in AGS.

(2) Feed composition

A variety of substrates have been successfully used for the cultivation of AGS,

including phenol, molasses, acetate, ethanol, starch, sucrose, glucose and other synthetic wastewater components (Adav et al., 2007; Liu and Tay, 2004; Moy et al., 2002a; Sun et al., 2006; Tay et al., 2005; Zheng et al., 2006). There are also reports on AGS cultivation by using the actual wastewater (Wang et al., 2007).

(3) Food to microorganism ratio (F/M) or organic loading rate (OLR)

F/M ratio or biomass-based organic loading rate (OLR) is an important parameter relating to the formation of AGS. A higher F/M ratio is helpful to promote the rapid formation of larger particles, and to enhance particle stability and increase particle size (Lobos et al., 2008). Similarly, volumetric OLR is another useful operating parameter that controls the formation of AGS. AGS can be cultivated at lower or higher OLR conditions (2.5-15 kg chemical oxygen demand (COD)/m^3·d) (Liu et al., 2003a; Moy et al., 2002a). It has been shown that aerobic granulation can achieve higher OLRs with simple substrates such as glucose and acetate.

(4) Metal ions

According to previous studies, metals (Ca^{2+}, Mg^{2+}, and zerovalent iron (ZVI)) in synthetic wastewater can reduce the time required to form AGS (Kong et al., 2014; Sarma et al., 2017). These metals can promote aerobic granulation in the following ways: i) promote the adhesion between microorganisms by reducing the negative charge on the surface of microbial cells; ii) promote the production of EPS; and iii) act as a nuclear attachment formation for bacteria aggregates. Addition of Ca^{2+}, Mg^{2+} or ZVI can neutralize the negative charge of microbial cells to assist bacterial aggregation. Multivalent cations accelerate the formation of AGS, and the formed particles may have a denser and denser microbial structure. Cai et al. (2018) found that a constant Fe^{2+} dosage strategy is conducive to the growth of biomass, resulting in aggregates with higher biological activity. On the other hand, the dosage strategy of pulsed Fe^{2+} can promote the granulation process and enhance the physical structure of the particles (Cai et al. 2018). Similarly, Yilmaz et al. (2017) also found that iron ions (Fe^{2+}/Fe^{3+}) increased the size and stability of AGS but did not affect the granulation time. The metal cations can increase the production and metal interactions of EPS, and then improve the microbial aggregation, formation and stability of AGS.

(5) Hydraulic retention time (HRT) and solids retention time (SRT)

Hydraulic retention time (HRT) is also an important parameter in the process of AGS formation. The hydraulic conditions in the reactor and the contact time between different reactants are affected by HRT. HRT should be carefully selected to optimize reactor performance. HRT of 6 h is reported to be the most conducive to the formation of AGS

(Pan et al., 2004). At an SRT of longer than 30 days, it was not possible to remove enough sludge from the system to keep a low phosphate concentration in the treated water (Ni et al., 2010). The biomass content might increase with the increase of SRT, but the ratio of active biomass decreased (Ni et al., 2010).

(6) Settling time

The settling time (i.e., granules that can settle down in a given period of time) should be applied to the sludge particles in the system, and the sludge that cannot settle down in the specified time will be washed away from the reactor (Qin et al., 2004). Compared with other factors such as sludge retention time (SRT), the minimum settling velocity can create a hydraulic selection pressure in favor of aerobic granulation in SBR (Li et al., 2008).

(7) Hydrodynamic shear force

The high shear force is conducive to agglomerates formation by microorganisms and accelerates the granulation process, thereby forming AGS with high particle stability (Beun et al., 1999). Moreover, a higher superficial gas flow rate makes the diffusion limitation not adversely affect the operation of the reactor and the formation of AGS, which in turn facilitates the formation of smaller and denser AGS (Tay et al., 2001).

(8) Configuration of reactor

Reactors with low ratio of height to diameter (H/D) values tend to form heterogeneous flow patterns through granular beds. However, a larger H/D ratio can provide stronger hydraulic conditions and more stable circulating flow, which can provide better DO and matrix mass transfer and mixing conditions, then can quickly form granular sludge with a dense structure. The shear rate in the granular reactor with a larger ratio of H/D was higher than that in the reactor with smaller H/D. However, the sequencing airlift bioreactor with smaller H/D can also have a high shear rate under the same superficial gas velocity (Zhu et al., 2014).

1.4.3 Mechanisms involved in AGS formation

The formation of AGS involves intercellular adhesion, which includes biological and physiochemical phenomena, is now attracting more and more attention (Zheng et al., 2006). Under aerobic or aerobic-anaerobic conditions and without adding any carrier material, AGS is formed by immobilizing microorganisms (especially bacteria) by themselves (Adav et al., 2008). There are two types of bacterial aggregation: auto-aggregation (intercellular interactions that inherit the same strain) and co-aggregation (intercellular adhesion between genetically different bacterial partners) (Khan et al.,

2013). Flocs adhere to the surface of crushed particles to reduce sludge loss, maintain nutrient removal during granulation, and quickly form AGS. Four different stages for the formation of AGS are proposed, including i) the contact between cells, ii) aggregates formed by the attachment of microorganisms, iii) EPS excretion to enhance attachment, and iv) hydrodynamic shear forces to shape the granules (Nancharaiah and Kiran Kumar Reddy, 2018).

The operating conditions of the reactor, including the shear force and the periodic feast-famine condition, are conducive to the induction of EPS excretion and the formation of compact and dense AGS (Lv et al., 2014). In addition, the short settling time facilitates the discharge of flocs with poor settling properties, thereby allowing fast settling particles to remain in the reactor. Further research is still necessary to clarify the mechanisms related to EPS secretion and microbial aggregation in order to further understand the formation mechanisms of AGS.

1.4.4 Applications of AGS in wastewater treatment

AGS biotechnology has been widely used to remove organic carbon, nitrogen, phosphorus, trace and refractory pollutants, and heavy metals due to its many advantages: high removal efficiency, good settleability, resistance to impact and toxins, longer SRT (Anuar et al., 2020; Coma et al., 2012; Hamiruddin et al., 2019).

(1) Nitrogen and phosphorus removal

The microbial respiration and diffusion limitation in the outer layer of AGS make the millimeter-sized AGS have aerobic and anoxic/anaerobic microenvironments. During the aeration process, the simultaneous nitrification and denitrification processes can occur inside the AGS at the same time, which is due to the existence of different redox conditions inside the granules (Coma et al., 2012; Nancharaiah et al., 2016). Due to the coexistence of aerobic and anoxic regions, nitrification and denitrification are carried out simultaneously in large granules under the same reactor operating conditions. In the AGS reactor, nitrate can be successfully denitrified. In addition, the use of acetate as an electron donor can achieve effective reduction of high-strength nitrate (Suja et al., 2015). Jiang et al. (2003) found that there were similar heterotrophic nitrifying microbial populations, and simultaneous nitrification and denitrification were also observed in AGS by Beun et al. (2001). In addition, DO concentration has a significant effect on the denitrification efficiency of AGS.

Many studies have shown that the P in wastewater can be effectively removed by the AGS reactor (Barr et al., 2010a; Barr et al., 2010b). With the increase of P/COD ratio in

the substrate, the accumulation of phosphorus showed a downward trend. When using AGS to treat slaughterhouse wastewater in SBR, > 98% of COD and P, and > 97% of N and volatile suspended solids (VSS) can be removed (Cassidy and Belia, 2005). He et al. (2018) achieved efficient and stable removal of carbon and phosphorus in the AGS system, improved nitrogen removal was realized at a reduced aeration time.

(2) Degradation of toxic organic substances

Phenol, which is toxic to aquatic organisms, has been successfully degraded by AGS (Chung et al., 2003; Tay et al., 2005). By feeding synthetic wastewater containing phenol as the sole carbon source, AGS that can degrade phenol is cultivated from AS (Jiang et al., 2004). A phenol degradation rate of 1.18 g phenol/g-VSS·d was achieved by AGS (Adav et al., 2007). AGS can also achieve biodegradation of up to 1000 mg/L phenol (Adav et al., 2007; Jiang et al., 2004). The mass transfer barrier caused by the large volume of AGS makes the local phenol concentration on the cell lower than the value in the solution, which may be a possible reason for the higher degradation efficiency of the phenol-degrading AGS (Liu and Tay, 2004). Jiang et al. (2004) found that *β-proteobacteria* and high G + C Gram-positive bacteria dominated in the phenol-degrading AGS. It is reported that when supplied with acetate, AGS is suitable for removing toxic chlorophenols such as 4-chlorophenol or 2,4,6-trichlorophenol (Carucci et al., 2009). In addition, the toxic 2-fluorophenol in synthetic wastewater can also be effectively treated by the AGS reactor (Duque et al., 2011). AGS can efficiently degrade pyridine (200 – 2500 mg/L) which is a by-product of coal gasification and utilized as a catalyst in the pharmaceutical industry (Adav et al., 2007; Stuermer et al., 1982). Phenol degrading AGS can simultaneously degrade phenol and pyridine (Adav et al., 2007).

(3) Metal and radionuclide contaminants removal

AGS can also be used as an efficient biosorbent for removing metals and radionuclide contaminants due to that metal-loaded AGS has good settling properties and can be easily separated from aqueous solutions (Yarlagadda et al., 2006). In addition, all kinds of wastewater including domestic sewage often contain metal contaminants. The metals in wastewater can affect biotransformation even in the range of a few micrograms per liter, especially the removal of nitrogen and phosphorus. AGS has been applied to the removal of Cd (II), Cu (II), Zn (II), Ni (II) and U (VI) from water (Liu et al., 2015b; Nancharaiah et al., 2006b). The initial concentrations of the copper (II) and zinc (II) in the reactor have been determined as one of the important factors affecting the maximum biosorption capacity of individual copper (II) and zinc (II) by AGS (Xu et al., 2004). Liu et al. (2005) found that carboxyl and hydroxyl groups were involved in metal adsorption.

1.4.5 Applications of AGS in Cr-containing wastewater treatment

As a biological adsorbent, AGS has been applied to Cr (VI) adsorption treatment. For instance, Sun et al. (2010) found that the absorption capacity of the polyethyleneimine-modified AGS was about 401.5 mg/g at pH 5.5, which increased by 274% compared to the control, and the adsorption process was pH dependent. In addition, the biotransformation and immobilization of Cr (VI) by AGS has been proven with complete 0.2 mM Cr (VI) removal in 2 - 6 days (Nancharaiah et al., 2010; Nancharaiah et al., 2012). On the other hand, Chen et al. (2018) found that 0.5 M $NaHCO_3$ was the best desorbent. The desorption rate of Cr (VI) was 62%, and the desorption rate of Cr (III) was 10%, which negatively affected the stability of the granules to some extent.

1.4.6 Research gap and problems statement

Although AGS has been attempted for Cr (VI) removal from wastewater, and the adverse effect of Cr (VI) on the AGS system has been extensively studied, there are very few studies to remove or mitigate this adverse effect. If left untreated, the accumulation of adverse effects caused by Cr (VI) will lead to the collapse of the whole AGS system. This study is the first trial to propose the use of a dynamic adsorption/desorption process to solve the adverse effects of Cr (VI) on the AGS system. It remains unknown the optimal parameters involved in the operation process that will affect the performance of the AGS system. The physical and chemical properties of granular sludge during the desorption process and its response to the desorption process are still not clear. Therefore, it is both a challenge and an opportunity for us to study the dynamic adsorption/desorption process of Cr (VI) on AGS, in order to realize the recycling of AGS and heavy metals, and maintain the basic function of AGS to remove pollutants during long-term operation.

1.5 Objectives of this research and thesis structure

The objectives of this research are: (1) to explore the changes of physical and chemical properties of AGS during adsorption/desorption using batch experiments; and (2) to explore the effects of dynamic adsorption/desorption process on the AGS system with the respect of bioactivity, pollutants removal efficiency and changes of EPS secretion.

The thesis structure is displayed in Fig. 1-1. This thesis is divided into 5 chapters. In Chapter 1, based on the literature review, the research background and significance are proposed. Firstly, the existing environmental problems and the more prominent chromium heavy metal pollution problems and treatment methods are introduced. Then the

introduction is focused on the physical and chemical characteristics, cultivation, and formation mechanism and application status of AGS. At last, the goal and framework of the paper are proposed.

In Chapter 2, the effects of desorption operation parameters, including kinds of desorbent, their concentration and contact time on AGS bioactivity and stability were investigated. Two kinds of kinetics model were also used to fit the desorption data.

In Chapter 3, the performance comparison among different reactors with or without dynamic adsorption/desorption was conducted, and the effects of different desorbed biomass proportion and desorption frequency on AGS system were investigated with respect to Cr (VI) and nutrients removal as well as biochemical characteristics of AGS.

In Chapter 4, three SBRs were used to investigate the effect of different OLRs (0.5, 1 and 2 kg COD/m^3·d) on the bioactivity and physicochemical characters of AGS under dynamic adsorption/desorption operating model. Some parameters, including specific oxygen uptake rate (SOUR), integrity coefficient, mixed liquor volatile suspended solids (MLVSS), settling velocity, size and morphology, were investigated to evaluate the impact of different OLRs on AGS.

At last, in Chapter 5, the main conclusions are summarized with the future research directions being proposed.

Table 1-1. Sources of different heavy metals (Paul, 2017).

Heavy metal	**Sources**
Arsenic (As)	Pesticides, fungicides, metal smelters
Cadmium (Cd)	Welding, electroplating, pesticies, fertilizer, betteries, nuclear fission plant
Chromium (Cr)	Minig, electroplating, textile, tannery industries
Copper (Cu)	Electroplating, pesticides, mining
Lead (Pb)	Paint, pesticides, batteries, automobile emission, mining, burning of coal
Manganese (Mn)	Welding, fuel addition, ferromanganese production
Mercury (Hg)	Pesticides, batteries, paper industries
Nickel (Ni)	Electroplating, zinc base casting, battery industries
Zinc (Zn)	Refinerise, brass manufacture, metal plating, immersion of painted idols

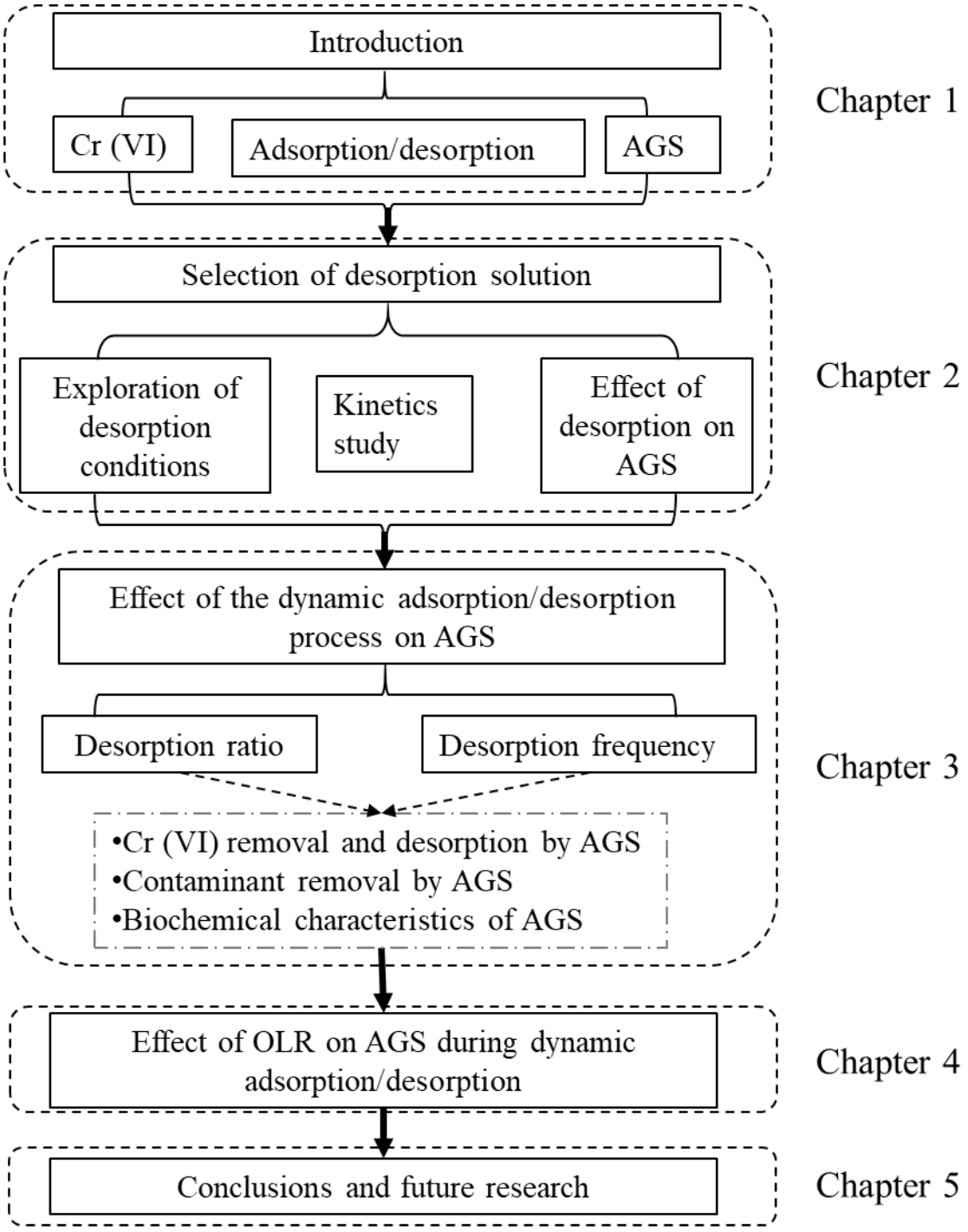

Fig. 1-1. The framework of this study. AGS: aerobic granular sludge, Cr (VI): hexavalent chromium, OLR: organic loading rate.

Chapter 2 Desorption of hexavalent chromium from active aerobic granular sludge: Effects of operation parameters on granular bioactivity and stability

2.1 Introduction

With the rapid globalization and industrialization, more than tens of thousands of factories relating to stainless steel, electroplating, leather tanning, fertilizer and pesticide industry are in operation worldwide. Due to the less stringent emission standards and random discharge of effluents from factories, domestic wastewater usually contains some amount of heavy metals (HMs) such as Hg, Cr, Pb, Cd, As, etc. (Anyanwu et al., 2018; Mahmood et al., 2012). Without proper treatment, HMs-containing wastewater can cause carcinogenesis and mutation, posing a real threat to human health (Talaiekhozani and Rezania, 2017). Hexavalent chromium (Cr (VI)) is one of the most common environmental HMs in wastewater and must be properly treated before being discharged to natural water bodies due to its high toxicity to all forms of living organisms, mutagenicity and/or carcinogenicity to bacteria, humans and animals (Dhal et al., 2013; Habibul et al., 2016; Losi et al., 1994). Among the various technologies for Cr (VI) removal, adsorption possesses great potential for Cr (VI) removal from wastewater due to the wide availability and low cost of adsorbents. Khosravi et al. (2018) used green nanocomposite derived from Harmala seed to adsorb chromium from aqueous solution, achieving a maximum adsorption capacity (Qm) of 53.48 mg/g. Using *E.coli* supported kaolin, Quiton et al. (2018) obtained achieved 91.00 mg/g of Cr (VI) adsorption capacity of Cr (VI). Meanwhile, the Cr (VI) adsorption capacity can reach 99.43 mg/g by tobacco petiole biochar from pyrolysis at 300 °C (Zhang et al., 2018). However, both adsorption and desorption processes should be considered for the adsorbent at the same time, since it`s still a challenging issue to deal with the Cr-loaded sorbents. Selection of an appropriate desorption solution (desorbent) is important and crucial for the regeneration and safe disposal of the adsorbent. An efficient desorbent is expected to completely desorb Cr (VI) without destroying the structure and functional groups of the adsorbent. Up to the present, various desorbents including HCl, HNO_3, NaOH, $NaHCO_3$, and Na_2CO_3 have been used for the desorption of Cr (VI) from the biomass of bacteria, fungi, microalgae, and aerobic granular sludge (AGS) as shown in Table 2-1 (Chen et al., 2018a; Jayakumar et al., 2015; Rezaei, 2016; Sudha Bai and Abraham, 2003).

AGS is a form of microbial auto-aggregation under aerobic condition without supporting carriers, which has been considered as one of the most promising biotechnologies for wastewater treatment (Wang et al., 2018). Due to its compact structure and high biomass retention, AGS exhibits good sedimentation performance and strong resistance to toxicants and recalcitrant pollutants such as phenol, azo dyes and metal contaminants, thus has been widely used for adsorption tests to remove various toxic and harmful pollutants including refractory toxic biological compounds and metal ions (Nancharaiah and Kiran Kumar Reddy, 2018). However, most of the previous adsorption trials using AGS as adsorbent are mainly on adsorption, paying little attention to desorption (Nancharaiah et al., 2012; Sun et al., 2011). Moreover, previous adsorption/desorption experiments were usually carried out under extreme conditions, such as strong acidic and alkaline conditions. Few of them concentrated on neutral condition within the pH range of domestic wastewater. Furthermore, very limited information is available on the bioactivity and stability of AGS during the adsorption and desorption processes (Chen et al., 2018a; Sun et al., 2011). As it is known, the granular stability and bioactivity after desorption is also important to maintain the AGS performance on organics and nutrients removal for long-term aerobic granule processes in addition to HMs adsorption, due to the fact that a relatively long time is necessary for the formation of AGS which is mainly composed of slowly growing bacteria. Restated, desorption process is conducive to the continuous operation of AGS wastewater treatment system, the reduction of operating costs, the Cr (VI) recovery and safe disposal of exhausted AGS (Jayakumar et al., 2015; Singha and Das, 2011).

In this work, Cr (VI) adsorption onto AGS was performed under neutral conditions to mimic the actual operation of AGS system, and then focused on desorption by various desorbents including sodium carbonate (Na_2CO_3), sodium bicarbonate ($NaHCO_3$), disodium phosphate (Na_2HPO_4), sodium sulfate (Na_2SO_4) and phosphate buffer saline (PBS) considering that they contain divalent anions or their aqueous solutions tend to be alkaline which may be beneficial for the desorption of Cr (VI). The effects of desorption on AGS bioactivity and granular stability, cations release and changes in extracellular polymeric substances (EPS) from AGS were explored to shed light on the mechanisms involved. In addition, the pseudo-first-order and pseudo-second-order kinetic models were used to estimate the maximum desorption capacity and reveal the desorption kinetics.

2.2 Materials and methods

2.2.1 AGS preparation

The AGS cultivated in a lab-scale sequencing batch reactor (SBR, mother cultivation reactor) using synthetic domestic wastewater for more than two years was used for Cr (VI) sorption and subsequent desorption experiments after moisture being removed or adsorbed and weighted. Granules with an average granular size of 0.89 ± 0.48 mm were used in this study, which was determined by a stereo microscope (STZ-40TBa, SHIMADZU, Japan) with a program Motic Images Plus 2.3S (version 2.3.0).

2.2.2 Sorption experiments

The batch adsorption experiments were carried out in 300 mL Erlenmeyer flasks under 1 h no-aeration and 5 h aeration to simulate a six-hour operation cycle of the mother SBR cultivation. Each flask was filled with 125 mL tap water, 125 mL Cr (VI) containing synthetic wastewater and 20 g wet AGS. The composition of Cr (VI)-containing synthetic wastewater was: 25 mg Cr (VI) /L ($K_2Cr_2O_7$), 500 mg chemical oxygen demand (COD)/L (CH_3COONa), 50 mg NH_4^+-N/L (NH_4Cl), 5 mg PO_4^{3-}-P/L (KH_2PO_4), 250 mg/L $NaHCO_3$,10 mg Ca^{2+}/L ($CaCl_2 \cdot 2H_2O$), 0.5 mg Fe^{2+}/L ($FeSO_4 \cdot H_2O$), 5 mg Mg^{2+}/L ($MgSO_4 \cdot 7H_2O$), and 1 mL trace metal elements solution (Moy et al., 2002b). The synthetic wastewater was used without pH adjustment (pH around 7.5). After the adsorption experiment, the supernatant was sampled and filtered through 0.22 μm filter for analysis. The granules after Cr adsorption were named as Cr-loaded AGS and then were used for the subsequent desorption experiments.

The Cr (VI) adsorption capacity ($Q_{e,ads}$, mg/g) of AGS was calculated by determining the concentration of Cr (VI) in the solution before and after the adsorption process.

$$Q_{e,ads} = V (\rho_i - \rho_e) / M \quad (1)$$

where $Q_{e,ads}$ is the amount of Cr (VI) adsorbed onto per gram of AGS after 6 h sorption (mg/g); ρ_i and ρ_e are the initial and final Cr (VI) concentrations in the solution (mg/L), respectively; V is the initial solution volume (L) and M is the mass of volatile suspended solids of AGS (g).

2.2.3 Desorption experiments

The desorption experiments were conducted in 50 mL centrifuge tubes containing 3 g of wet Cr-loaded AGS and 45 mL desorption solution each. Then the mixture was

shaken at 150 rpm and room temperature for 60 min. The Cr (VI) desorption capacity ($Q_{e,des}$, mg/g) of AGS was calculated as follows:

$$Q_{e,des} = V \times \rho_{des} / M \quad (2)$$

$$DE\% = (Q_{e,des}/ Q_{e,ads}) \times 100 \quad (3)$$

where $Q_{e,des}$ is the amount of Cr (VI) desorbed from per gram of AGS (mg/g); ρ_{des} is the concentration of Cr (VI) in the desorbent solution (mg/L); V is the volume of desorption solution (L), and M is the mass of volatile suspended solids of AGS (g); DE% is the Cr (VI) desorption efficiency (%).

Each adsorption or desorption test was conducted in triplicate, and all the data were expressed as mean ± standard deviation (SD).

2.2.4 Effect of different salt or desorbent solutions

To investigate the effect of different desorbents on desorption efficiency, five different salt solutions including sodium carbonate (Na_2CO_3), sodium bicarbonate ($NaHCO_3$), disodium phosphate (Na_2HPO_4), sodium sulfate (Na_2SO_4) and phosphate buffer saline (PBS) were examined as desorbent with H_2O as the control. 0.25 M of each desorbent was tested in the desorption experiments. Except for the type of desorbent, all the other variables were the same, and the desorption experiments were carried out as described in section 2.3.

2.2.5 Effect of different desorbent concentration and contact time

Different concentrations of Na_2CO_3, i.e. 0.1, 0.25, 0.5 and 1 M were prepared to investigate the effect of different concentrations of desorbent on desorption efficiency, cations release and EPS change in the AGS in addition to its bioactivity and stability. The desorption experiments were conducted as in section 2.3.

Specifically, in the experiments relating to the effect of contact time on desorption efficiency, cations release from AGS, and granular bioactivity and stability, the samples were taken at designated intervals between 5 and 180 min and then Cr (VI) concentration in the solution was determined. In this study, the pseudo-first-order and pseudo-second-order kinetic models were used to analyze the desorption data. Except for the contact time, all the other operation conditions remained unchanged, and the desorption experiments were carried out as described in section 2.3.

2.2.6 Analytical methods

Cr (VI) concentration was measured using a UV/vis spectrophotometer (UV 1800, Shimadzu, Japan) at the wavelength of 540 nm. pH was measured by a portable pH meter (model AS600, China). The concentrations of cations such as Ca^{2+}, Mg^{2+}, and K^{+} were determined by Liquid Chromatography (Shimadzu, Japan). Proteins (PN) and polysaccharides (PS) in the extracted EPS (with the heating method) were quantified by using Bradford method and phenol-sulfuric acid method with bovine serum albumin (BSA) and glucose as the standard, respectively (Bradford, 1976; DuBois et al., 1956). In this study, the microbial activity and stability of AGS were expressed in terms of specific oxygen uptake rate (SOUR) and integrity coefficient as described previously (Chen et al., 2018a). To be specifically, the latter was determined as the ratio of solid weight in the supernatant after being shaken on a shaker at 200 rpm for 5 min to the total weight of the AGS (Ghangrekar et al., 2005).

2.3 Results and discussion

2.3.1 Cr (VI) adsorption capacity of AGS under neutral condition

After 6 h adsorption, the Cr (VI) adsorption capacity ($Q_{e,ads}$, mg/g) of the test AGS was 0.57 ± 0.04 mg/g-VSS, which is remarkably lower than the results from previous works including our own research (Chen et al., 2018a). This difference could be attributable to the relatively low initial Cr (VI) concentration in the reactor (12.5 mg/L when influent Cr (VI) was 25 mg/L), short contact time (only 6 h), neutral (pH ~ 7.5) and aerobic conditions (5 h aeration). Also, the concentration of trivalent chromium (Cr (III)) as a reduction product of Cr (VI) was determined in the effluent during the desorption process. It was found that Cr (III) was almost undetectable in the supernatant (data not shown), which should be further researched in the followed-up experiments. In the subsequent desorption tests, only Cr (VI) was concerned.

2.3.2 Effect of different desorbent solutions

It is expected that after desorption, the adsorbents can be reused for multiple times for the continuous operation of AGS system, resulting in the reduction of costs for adsorbent processing and supply, and exhausted adsorbent disposal (Gupta and Rastogi, 2008). In this study, five different desorbents were examined to study the desorption of Cr (VI) from AGS (Fig. 2-1a). As shown, the desorption efficiency with H_2O as the

control was around 19.63 ± 0.032%, and Na_2CO_3 solution reflected the best desorption efficiency of 24.59 ± 0.29% among all the test desorbents. This observation is probably associated with the alkaline condition of Na_2CO_3 solution, in which the existing form of Cr (VI) is CrO_4^{2-} (Daneshvar et al., 2017). This alkaline condition may result in more negatively charged sites on the surface of AGS thus some improvement of Cr (VI) desorption efficiency due to the electrostatic repulsion between anionic Cr (CrO_4^{2-}) and negatively charged sites on the AGS (Daneshvar et al., 2017; Nancharaiah and Kiran Kumar Reddy, 2018). Another reason may be associated with the large amount of OH^- (around $1\times10^{-2.9}$ M based on pH 11.1) and CO_3^{2-} (around 0.25 M) ions in the alkaline solution and their exchange with CrO_4^{2-} ions on the AGS (Chen et al., 2018a; Otero et al., 2015). Therefore, the desorbent solution with more anions is generated in the desorption process, especially hydroxide ions (OH^-), which are more effective for the desorption of metal anions from HM-loaded adsorbent. It can also be seen that, as a commonly used cell cleaning and culture solution (Nakai et al., 2016), PBS can achieve the lowest desorption efficiency of 11.14 ± 0.02%. In addition, when all the solution pHs of the five desorbents being adjusted by adding KH_2PO_4 to around pH 7.41 ± 0.09, their desorption efficiencies decreased significantly to < 15%, especially for Na_2CO_3 solution (only 10.85 ± 0.46%), indicating that the desorbent pH might be the major factor influencing Cr (VI) desorption from Cr-loaded AGS.

2.3.3 Effect of desorbent concentration and contact time

Fig. 2-1b shows the effect of contact time and Na_2CO_3 concentration (0.1 - 1 M) on Cr (VI) desorption efficiency from Cr-loaded AGS with H_2O as the control. It was found that the desorption efficiency was improved with the increase in Na_2CO_3 concentration. The highest desorption ratio, 33.65 ± 0.76% was obtained when 1 M Na_2CO_3 was applied, with the lowest performance (15.18 ± 0.72%) achieved by using H_2O. As shown in fig. 2-1c, the increase of Na_2CO_3 concentration will lead to the increase of OH^- (according to the increasing pH) and CO_3^{2-} concentrations, resulting in the increase of Cr (VI) desorption efficiency owing to the competition among OH^-, CO_3^{2-} and chromium anions (CrO_4^{2-}) for the adsorption sites on the AGS surface and the repulsive force of negatively charged AGS after loading OH^-, CO_3^{2-} to chromium anions (CrO_4^{2-}) (Otero et al., 2015). Singha and Das (Singha and Das, 2011) found that with the increase of NaOH concentration from 0.05 M to 0.50 M, the percentage of Cr (VI) desorption from biomass increased from around 10.24 ± 3.35% to 20.02 ± 2.31%. The results from this work agree with our previous study (Chen et al., 2018a), in which the desorption efficiency of Cr (VI)

from AGS increased with the increase in Na_2CO_3 concentration, achieving the highest desorption ratio of 38.03% by using 0.5 M Na_2CO_3 under the designed conditions.

In addition, for all the test desorbent solutions except H_2O, the desorption of Cr (VI) was very fast during the first 60 min, and then gradually increased until 180 min, which is most probably due to the highest concentration gradient at the initial stage. Along with the desorption, Cr concentration in the solid phase decreases while Cr concentration in the liquid phase increases, thus the opposite may also occur. Interestingly, when H_2O is used as desorbent, Cr (VI) desorption efficiency increased during the first 60 min, then decreased in the later 60-120 min, possibly due to the Cr-desorbed AGS may quickly recover its adsorption potential as little adverse effect on the bioactivity of AGS exerted by H_2O (Fig. 2-3a).

2.3.4 Kinetics study

Desorption kinetics is important for adsorbent design and regeneration, which is also necessary for selection of the best desorbent and its operation conditions in the real practice (Daneshvar et al., 2017). In the present study, the desorption data were used to fit the pseudo-first-order and pseudo-second-order kinetic equations, which have been applied to desorption process in previous study (Daneshvar et al., 2017). Their linear form equations can be written as Eqs. (4) and (5), respectively (Li et al., 2013):

$$\log\left(Q_{eq,des} - Q_{t,des}\right) = log\, Q_{eq,des} - \frac{K_1}{2.303}t \quad (4)$$

$$\frac{t}{Q_{t,des}} = \frac{1}{K_2 Q_{eq,des}^2} + \frac{t}{Q_{eq,des}} \quad (5)$$

where t is the desorption time (min); K_1 (1/min) and K_2 (g/(mg·min)) are the rate constants for the pseudo-first-order and pseudo-second-order models; $Q_{t,des}$ and $Q_{eq,des}$ (mg/g) are the desorption amount at desorption time t and equilibrium state, respectively.

Fig. 2-2a and b plot the kinetic curves for Cr (VI) desorption with Na_2CO_3 solution as desorbent, and the related experimental data and the model parameters estimated are summarized in Table 2-2. Based on the experimental data, the correlation coefficient (R^2 = 0.9849–0.9947) for the pseudo-second-order equation is much higher than that for the pseudo-first-order model (R^2 = 0.7057-0.9879), especially under lower Na_2CO_3 concentration condition. In addition, the calculated values of $Q_{eq,des}$ from the pseudo-second-order model are nearly approximate to the experimental data, suggesting that the pseudo-second-order equation is more suitable for the prediction of equilibrium desorption capacity than the pseudo-first-order one. This observation also means that the

desorption process is more likely a physicochemical desorption process which may involve the substitution of CO_3^{2-} for CrO_4^{2-} to form chemical bonds with functional groups including PN, PS, glycoproteins, glycolipids, etc. on the granule surface, which might be the limiting step (Jobby et al., 2018). Further research is necessary for more proofs to confirm the mechanisms involved.

2.3.5 Effect of desorption on the bioactivity and stability of AGS

Maintenance of high granular bioactivity and stability is crucial for the continuous operation of AGS system to remove target pollutants. The effects of Cr (VI) adsorption and desorption by different Na_2CO_3 concentration (0.1-1 M) on SOUR and integrity coefficient were studied.

As seen from Fig. 2-3a, the granular SOUR decreased from initial 22.38 ± 1.37 mg-O_2/g-VSS·h to 14.37 ± 0.34 mg-O_2/g-VSS·h after Cr (VI) being adsorbed or loaded, most probably attributable to the inhibition effect on bioactivity brought about by the high Cr (VI) concentration (25 mg/L in the influent) (Kiran Kumar Reddy and Nancharaiah, 2018; Zheng et al., 2016). While Cr (VI) adsorption seemed to have limited impact on granular stability as the integrity coefficient only slightly increased from 5.52% to 6.42% (Fig. 2-3a), which is consistent with the finding by Chen et al. (2018). The desorption with H_2O as the control showed slightly negative effect on the bioactivity as indicated by SOUR (12.68 ± 0.53 mg-O_2/g-VSS·h).

Generally, the granular stability of AGS was impacted to some extent by using the test desorbents, including H_2O (integrity coefficient = 11.33%), with the greatest impact observed when 1M Na_2CO_3 was applied as the desorbent (SOUR = 5.55 ± 1.42 mg-O_2/g-VSS·h, Integrity coefficient = 25.63%). This phenomenon is closely associated with the relatively strong alkaline condition (pH = 12.07 ± 0.02 for 1M Na_2CO_3 solution) that is harmful to the microorganisms in AGS, leading to the decrease of bioactivity that is not conductive to the maintenance of the compact granular structure. The shaking condition applied for the desorption tests may make it worse. Restated, the relatively strong alkaline pH of Na_2CO_3 solution may be the major reason for the decreased granular bioactivity and stability.

The effect of contact time during desorption also has some impact on the SOUR and integrity coefficient. Fig. 2-3b shows the results by using 0.5 M Na_2CO_3 as the desorbent. As seen, the SOUR sharply decreased from 22.38 ± 1.37 mg-O_2/g-VSS·h to 9.09 ± 1.01 mg-O_2/g-VSS·h during the first 30 min contact, then the decrease trend slowed down and gradually to 6.99 ± 1.43 mg-O_2/g-VSS·h at 180 min. It has been reported that the cells on

the surface have higher respiratory activities and the entire granule can access to substrates, possibly through its inner channels and pores (Wang et al., 2018). While under strong alkaline desorption condition in this study, the aerobic and facultative bacteria located in the outer layer of the granules may first lose their bioactivity (Lv et al., 2014), thus the sharp decrease in SOUR was observed; and the inner part was less and later impacted due to the protective effect of its layered structure since a multilayer sphere structure can decrease substrate gradients from outside to the core of granular sludge (Wilén et al., 2018). The integrity coefficient was detected to sharply increase from 5.52% to 18.24% in the first 5 min, then continued to increase gradually to 23.81% at 180 min. This observation indicates that the compact granular structure was greatly affected at the first 5 min, and then gradually became looser and looser, which is in agreement with the change of granular bioactivity during the desorption process as the active bacteria play a key role in maintaining the structural and functional stability of AGS (Aqeel et al., 2019).

2.3.6 Effect of desorption on EPS

PN are distributed throughout the AGS, and nucleic acids and certain PS are mainly in the out layer of AGS (Wang et al., 2018). PN and PS are the two major components of EPS containing large amounts of functional groups such as hydroxyl and electronegative carboxyl, which are associated with the physicochemical properties of sludge during biological wastewater treatment (Guo et al., 2012; Zhu et al., 2012). EPS have been demonstrated to contribute to the removal of harmful substances (dye, CrO_4^{2-}, Cd^{2+}, Cr^{3+}, etc.) from aqueous environment and protect cells from harsh environments containing toxic metals and chemicals, such as Cd^{2+}, Cu^{2+}, Pb^{2+} and phenol, etc. (Fang et al., 2002; Liu et al., 2001). Fig. 2-4a represents the effects of Cr (VI) adsorption and desorption (by Na_2CO_3 solution) on the EPS of AGS. It is obvious that the Cr (VI) adsorption and desorption with H_2O as desorbent exerted little effect on the content of EPS (PN and PS), due to the short adsorption time (6 h) of Cr (VI) and the non-toxicity of water to AGS. With the increase of Na_2CO_3 concentration, PN rapidly increased from the initial 138. 17 ± 1.72 mg/g-VSS (Cr-loaded AGS) to 315.92 ± 5.98 mg/g-VSS (1 M Na_2CO_3), mainly from the increase of loosely bound PN (LB-PN) (data not shown). Meanwhile, the increment of PS was negligible (Fig. 2-4a). As a result, the PN/PS ratio increased from 5.21 ± 0.10 to 8.69 ± 0.70. Due to the fact that PN are more associated with sludge settleability and dewaterability than PS, the increase in PN content is beneficial for the maintenance of granular structure (Basuvaraj et al., 2015). Deng et al. (Deng et al., 2016) observed a similar phenomenon when the granules were under aerobic starvation: PN

were markedly secreted to protect the cells from the shock of adverse environment, which were supposed to supply to the microbes as domestic demand energy. It is well known that enzymes primarily consist of proteins. The increase of PN in EPS may be due to the secretion of a large quantity of enzymes to protect cells themselves from the influences of high alkaline environment (Li and Yang, 2007). More specifically, the increment of LB-PN is the main contributor to the increment of PN, accounting for about 78.03 ± 2.66%, possibly due to the fact that LB-PN is mainly distributed in the outer layer of AGS to resist the entry of external harmful substances (Sheng et al., 2010). As it is known, EPS excretion is the response of microorganisms to the external environmental conditions (Li and Yang, 2007). In summary, LB-PN are more sensitive to the increase of Na_2CO_3 concentration than tightly bound PN (TB-PN) and PS, and the significant increase of PN in EPS is mainly contributed by LB-PN.

2.3.7 Effect of desorption on cations release from AGS

The cations in AGS play an important role in maintaining the stability of AGS, especially Ca^{2+}, Mg^{2+} and K^+ (Wang et al., 2014a). A large amount of P and cations such as Ca^{2+}, Mg^{2+} and K^+ have been detected in EPS extracted from AGS (Wang et al., 2014a; Wang et al., 2014b). The change of cations in AGS after desorption should be studied because it is closely related to the function and stability of AGS. The effect of desorption by 0.1 M Na_2CO_3 solution on the variations of Ca^{2+}, Mg^{2+} and K^+ in the desorption solution was examined (Fig. 2-5a). A rapid increase in Ca^{2+}, Mg^{2+} and K^+ concentrations was detected in the desorption solution in the first 60 min, then slowed down and gradually increased to 9.18 ± 0.01 mg/L, 5.76 ± 1.76 mg/L and 19.6 ± 0.83 mg/L, respectively at 180 min, which is associated with the change of concentration gradient between the solid and liquid phases as reported by Daneshvar et al. (2017). Fig. 2-5a also reflects the typical extraction curve for the separation of substances from solid phase (Knez et al., 2013; Sovová, 2005), which generally consists of two periods: the first period for the fast release of loosely bound Ca^{2+}, Mg^{2+} and K^+, and the second one for the slower release of tightly bound Ca^{2+}, Mg^{2+} and K^+. In addition, the changes of Ca^{2+}, Mg^{2+} and K^+ concentrations during the desorption process by H_2O showed a similar trend but at small increments (data not shown).

The effect of different Na_2CO_3 concentrations on Ca^{2+} and Mg^{2+} release was also monitored. As seen from Fig. 2-5b, Mg^{2+} concentration increased with the increase of Na_2CO_3 concentration. The maximum Mg^{2+} concentration (10.40 ± 1.22 mg/L) was detected in the solution when 1 M Na_2CO_3 was used as desorbent, while H_2O desorption

had much less release of Mg^{2+} (0.70 ± 0.01 mg/L). Increase of Na_2CO_3 concentration results in the increase of CO_3^{2-} concentration which can promote the precipitation between Mg^{2+} and CO_3^{2-}. The different concentration gradient, on the other hand, may play a certain role in the transfer of Mg^{2+} from granules to the desorption solution. In the case of Ca^{2+}, it increased firstly and then decreased with the increase of Na_2CO_3 concentration, resulting from the balance between Ca^{2+} release and precipitation with CO_3^{2-}. The solubility product (K_{sp}) of the precipitate may determine the level of cations in the desorption solution. For example, $MgCO_3$ has a higher K_{sp} (1.93×10^{-4}) than $CaCO_3$ ($K_{sp}[CaCO_3] = 4.90 \times 10^{-9}$), thus more soluble Mg^{2+} should be remained in the desorption solution, especially under high Na_2CO_3 concentration conditions (0.5 and 1M Na_2CO_3 in this study). As Ca^{2+} and Mg^{2+} are important elements for bioactivity and granular strength, the loss of Ca^{2+} and Mg^{2+} in the AGS during desorption may negatively affect the stability, bioactivity and function of AGS.

Fig. 2-4b shows the variations of Ca^{2+}, Mg^{2+} and K^+ contents in the EPS after Cr (VI) adsorption and desorption by different concentration Na_2CO_3 solutions. Cr (VI) adsorption and desorption with H_2O as desorbent show little negative effect on the contents of Ca^{2+}, Mg^{2+} and K^+ in the EPS, except a slight decrease occurred in Ca^{2+} in H_2O desorption and a slight increase in K^+ in Cr-loaded AGS. The latter may be attributable to the higher K^+ concentration in the AGS due to the use of $K_2Cr_2O_7$ for influent preparation. It was noticed that desorption process using Na_2CO_3 led to a significant decrease of Ca^{2+}, Mg^{2+} and K^+ contents in the EPS. Compared to the initial AGS, increase of Na_2CO_3 concentration to 1 M can decrease Ca^{2+}, Mg^{2+} and K^+ contents in the EPS from 31.50 ± 1.71 mg/g to 0.58 ± 0.02 mg/g, from 13.18 ± 0.71 mg/g to 0.62 ± 0.02 mg/g, and from 41.38 ± 2.24 mg/g to 0.58 ± 0.02 mg/g, respectively. In addition, it was calculated that the reductions in Ca^{2+}, Mg^{2+} and K^+ in EPS accounted for 69.43%, 44.10% and 43.03% of the increases in Ca^{2+}, Mg^{2+} and K^+ concentrations in the 1 M Na_2CO_3 desorption solution, respectively, in which most of the released cations came from TB-EPS. The binding between EPS and divalent cations (such as Ca^{2+} and Mg^{2+}) is one of the main intermolecular interactions that maintain the stable structure of microbial aggregates (Mayer et al., 1999). Multivalent cations (such as Ca^{2+}, Mg^{2+}) tend to bridge with EPS, thereby improving flocculation of microbial aggregate (Higgins Matthew and Novak John, 1997; Liu et al., 2007). Therefore, the large loss of Ca^{2+}, Mg^{2+} and K^+ in EPS will inevitably lead to a decline in EPS function, including cell adhesion and protection, resulting in the reduction in biological activity and strength of AGS. Results from this study indicate that Na_2CO_3 solution can be used as desorbent for Cr-loaded AGS

at a lower concentration for a shorter contact time to alleviate the negative effect on AGS activity and granular strength in practice. More research works are necessary to seek out suitable desorbents and their applicable concentrations to maintain the granular bioactivity and stability when AGS is going through HMs adsorption/desorption and at the same time can maintain its normal operation performance on organics and nutrients removal. As it was noticed, after being desorbed, the AGS may regain its bioactivity and stability, and biosorption capacity to some extent after being soaked in a solution containing relatively high concentrations of Ca^{2+}, Mg^{2+}, and K^{+}, which is still under investigation.

2.4 Summary

In the present study, Cr (VI) desorption from Cr-loaded AGS was performed using five different desorbent solutions. Among them, the maximum desorption efficiency was determined as 33.65 ± 0.76% by 1 M Na_2CO_3. The results illustrate the occurrence of OH^- and CO_3^{2-} anions exchange with CrO_4^{2-} on the surface of AGS in the alkaline solution. The desorption behavior can be well described by pseudo-second-order model with a satisfactory determination coefficient (R^2 = 0.9849–0.9947). Cr (VI) desorption efficiency increased with the increase of Na_2CO_3 concentration and contact time, during which the granular bioactivity and stability were deteriorated as indicated by decrease in SOUR and increase in integrity coefficient. Loss of Ca^{2+}, Mg^{2+}, and K^{+} in the EPS (especially TB-PN) during the desorption process may be one of the major contributors to the deterioration of AGS bioactivity and stability. PN rather than PS were found to be more sensitive to the increased Na_2CO_3 concentration, especially the LB-PN. To reduce the negative effect on AGS activity and granular strength, results from this study indicate that Na_2CO_3 solution can be used as desorbent for Cr-loaded AGS at a lower concentration for a shorter contact time. In addition, after being desorbed, the AGS may regain its bioactivity and stability, and biosorption capacity to some extent after being soaked in a solution containing relatively high concentrations of Ca^{2+}, Mg^{2+}, and K^{+}, which is still under investigation.

Table 2-1. Comparison of Cr (VI) desorption performance by various desorbents prepared from different biomass.

Biomass	Desorbent	Cr (VI) desorption efficiency (%)	Reference
Aerobic granular sludge (AGS)	0.5 M $NaHCO_3$	64.45	Chen et al., 2018
	0.5 M Na_2CO_3	38.03	
Sargassum myriocystum (algae)	0.2 M HCl	97.21	Jayakumar et al., 2015
Spirulina sp. (bacteria)	0.1M HNO_3	95.04 ± 3.10	Rezaei, 2016
	0.1M EDTA	72.23 ± 3.15	
	0.1M HCl	89.57 ± 3.39	
Rhizopus nigricans (fungi)	0.01 M NaOH	87.91 ± 3.0	Sudha Bai and Abraham, 2003
	0.01 M $NaHCO_3$	89.14 ± 3.3	
	0.01 M Na_2CO_3	91.91 ± 3.9	

Table 3-2. Parameters estimated from the pseudo-first-order and pseudo-second-order models for Cr (VI) desorption from Cr-loaded AGS.

ρ_0	$Q_{eq,des}$[a]	Pseudo-first-order model			Pseudo-second-order model		
(Na_2CO_3)	(mg/g)	K_1	$Q_{eq,des}$[b]	R^2	K_2	$Q_{eq,des}$[b]	R^2
(mol/L)		(1/min)	(mg/g)		(g/(mg·min))	(mg/g)	
0.1	0.1516	0.0062	0.0444	0.7057	0.6909	0.1587	0.9849
0.25	0.1558	0.0094	0.0455	0.7406	0.8836	0.1567	0.9933
0.5	0.1727	0.0115	0.0607	0.9137	0.6801	0.1753	0.9947
1.0	0.2017	0.0154	0.0940	0.9879	0.4143	0.2097	0.9930

[a] $Q_{eq,des}$ is the experimental value.

[b] $Q_{eq,des}$ is calculated from the kinetic model.

(a)

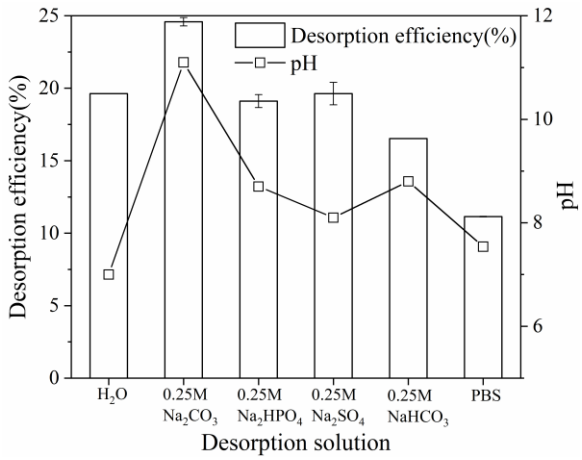

(b)

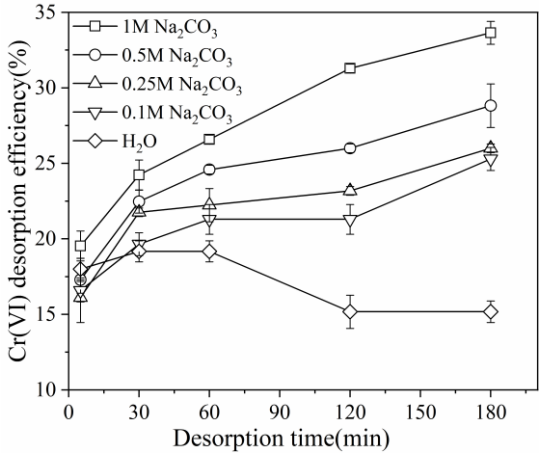

(c)

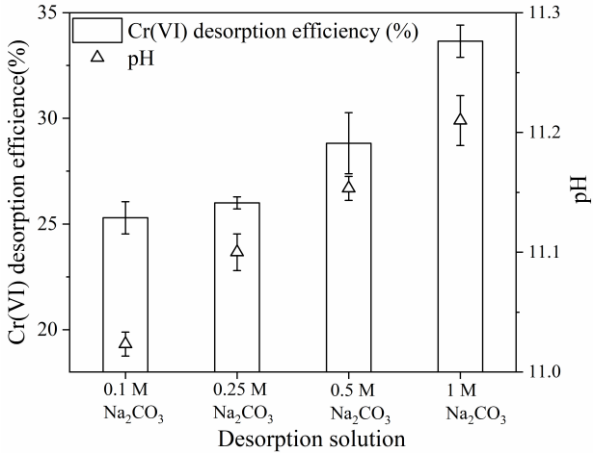

Fig. 2-1. Effects of different desorbents (a) and Na_2CO_3 concentrations (b) on Cr (VI) desorption efficiency from Cr-loaded AGS; the variation of pH and Cr (VI) desorption efficiency with the increase of Na_2CO_3 concentration (c).

(a)

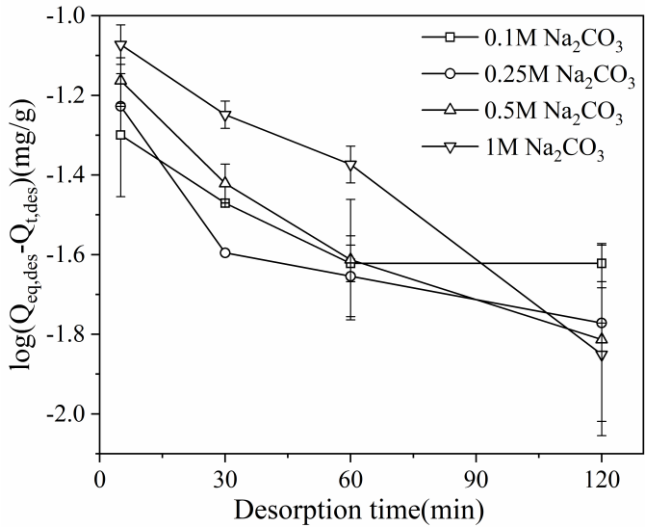

(b)

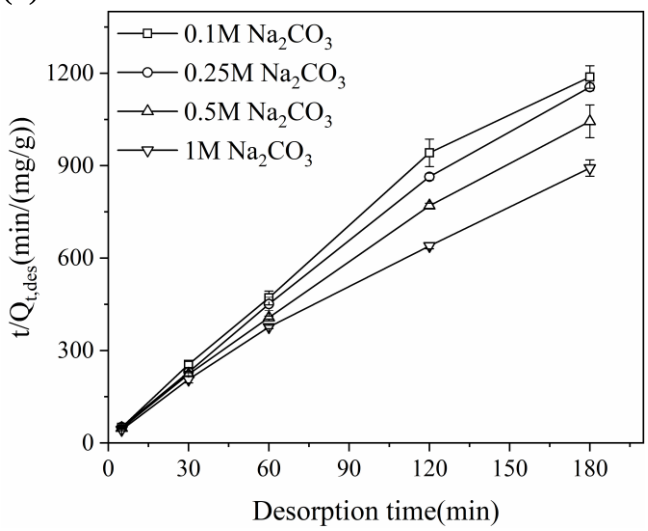

Fig. 2-2. The pseudo-first order (a) and pseudo-second-order (b) kinetic modeling for Cr (VI) desorption from Cr-loaded AGS.

(a)

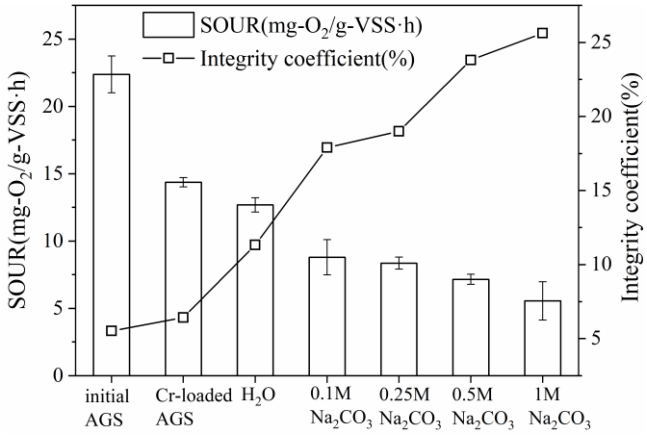

(b)

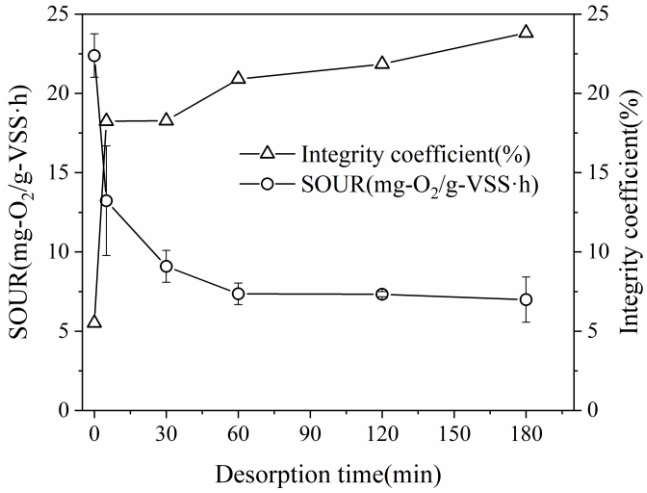

Fig. 2-3. Comparison of SOUR and integrity coefficient of initial AGS, Cr-loaded AGS and AGS after 60 min desorption (a), and changes of SOUR and integrity coefficient during the desorption process by 0.5 M Na_2CO_3 (b).

(a)

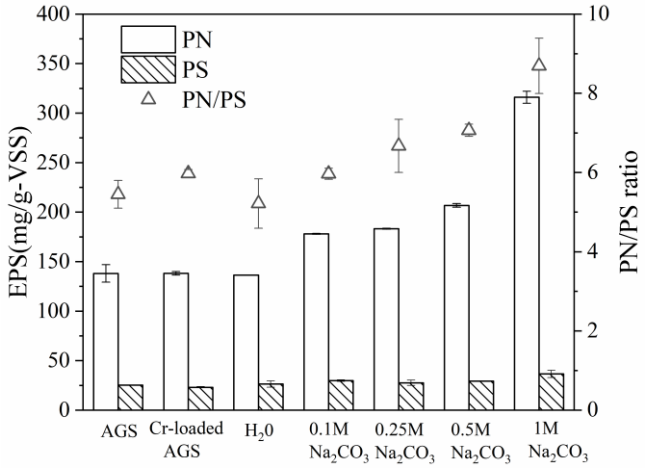

(b)

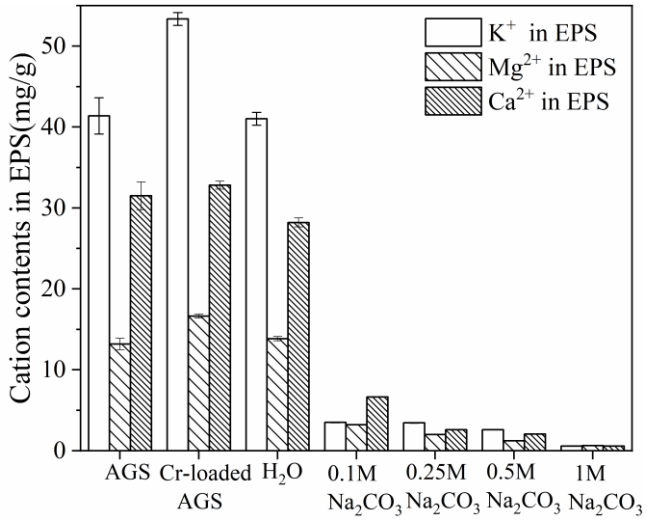

Fig. 2-4. Variations of EPS and PN/PS ratio of initial AGS, Cr-loaded AGS and AGS (a), and changes of Ca^{2+}, Mg^{2+} and K^{+} contents in EPS after 60 min desorption process (b).

(a)

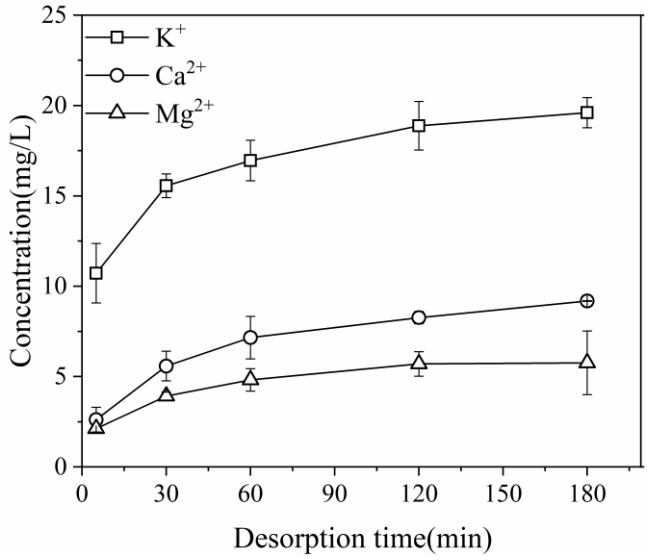

(b)

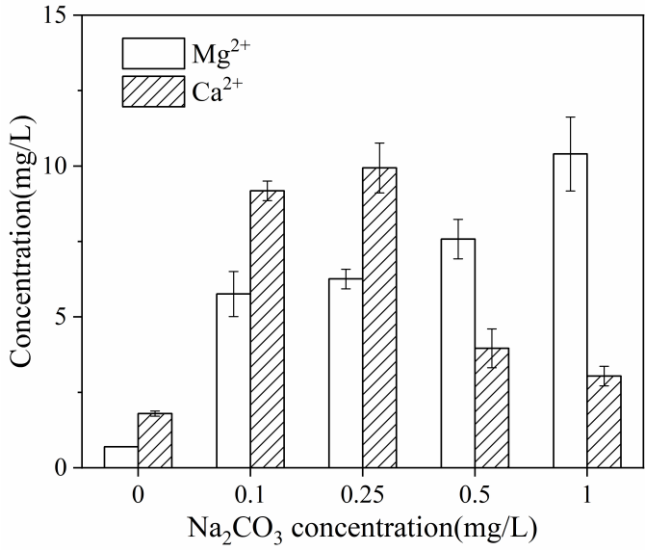

Fig. 2-5. Changes of Ca^{2+}, Mg^{2+} and K^{+} concentrations in solution during the desorption process with 0.1 M Na_2CO_3 as desorbent (a), and changes of the Ca^{2+} and Mg^{2+} concentrations in the solution after 60 min desorption process by different concentrations of Na_2CO_3 (b).

Chapter 3 Effect of the dynamic adsorption/desorption process on the removal of nutrients and Cr (VI) using AGS in SBR

3.1 Introduction

In Chapter 2, the effects of Cr (VI) desorption on the AGS bioactivity and stability have been investigated in batch tests. Results show that desorption can remove the chromium adsorbed on the AGS with slightly adverse effects. However, the effect of dynamic adsorption/desorption on AGS in SBR is unclear.

Therefore, in Chapter 3, six identical sequencing batch reactors (SBRs) were used to study the effect of dynamic adsorption/desorption on AGS from three aspects: with or without desorption, the ratio of desorption biomass, and the frequency of desorption. The experiments were divided into the three processes. In the first experiment, the reactor without Cr (VI) addition was used as the blank control group (R0), the reactor with Cr (VI) addition and no dynamic adsorption/desorption process was used as the control group (Rc), and the reactor with Cr (VI) addition and dynamic adsorption/desorption process (Ra/d) was used as the experimental group. Another two experiments were then followed under three different desorbed biomass proportion (25%, 50%, 75%) and desorption frequencies (1time/d, 1time/2d) to examine the SBR performance, including Cr removal, ammonia nitrogen removal, AGS bioactivity and stability, etc.

3.2 Materials and methods

3.2.1 AGS preparation and synthetic wastewater

AGS was domesticated from the activated sludge sampled from a local municipal wastewater treatment plant (WWTP) in Ibaraki, Japan and cultivated in one 1-L SBR in the laboratory for more than two years. AGS was used in the subsequent dynamic adsorption/desorption experiments of Cr after moisture being removed and weighted.

The composition of synthetic wastewater is the same as in section 2.2.2 except that the concentration of Cr (VI) was adjusted to 5 mg/L considering the low concentration of Cr (VI) in the actual domestic sewage and the high toxicity of Cr (VI). It should be noted that there was no Cr (VI) in the influent of the blank control group (namely R0).

3.2.2 Experimental setup

Six identical lab-scale plexiglass sequencing batch reactors with working volume of 250 mL each (internal diameter of 4.3 cm and effective height of 19.5 cm) were used in the dynamic Cr (VI) adsorption/desorption experiments. Six peristaltic pumps were used to feed the influent from the bottom with the effluent discharged from the middle of the reactor at a 50% volumetric exchange ratio. Aeration was supplied an airflow rate of 0.4 L/min by an air pump (AK40, KOSHIN, Japan) through a porous air diffuser at the bottom of the reactor, which is equivalent to 0.46 cm/s of air uplift velocity. The SBRs were operated at four cycles per day with each cycle for 6 h, including 4 min of influent filling, 60 min of non-aeration stage, 290 min of aeration stage, 2 min of settling, and 4 min of effluent discharge. Each cycle was automatically performed by the time controllers. The temperature of all the reactors was maintained at 20 ± 2℃. HRT was 12 h and SRT was controlled at 25 d by quantitative sludge discharge.

3.2.3 Sorption experiments

20 g of wet AGS was added to the SBR together with 125 ml tap water and 125 ml of synthetic wastewater through a peristaltic pump, and then the experiment was started under four cycles per day with 6 h for each cycle. At the beginning of a cycle, 125ml of Cr (VI)-containing influent water was pumped into the SBR for 6h adsorption, and then 125ml of effluent water was discharged at the end of the cycle to complete the Cr (VI) adsorption. The effluent in the first cycle after desorption was collected every day and placed in the refrigerator below 4 degrees Celsius after filtration with 0.22μm filter for storage and testing.

3.2.4 Desorption experiments

The desorption experiment started the day after the addition of Cr (VI) and was completed within 1.5 h at the end of one cycle. A fixed ratio of AGS was taken at a fixed time for desorption experiments. After the AGS being taken out, most of the free water was filtered through the filter screen, and then the water on the surface of the AGS and between the AGS was absorbed and removed by the filter paper. After the AGS being transferred to a 250 ml Erlenmeyer flask containing 100 ml 0.5 M Na_2CO_3, the mixture was shaken at 125 rpm under room temperature for 1 h. After the desorption, the supernatant was filtered through a 0.22 μm filter membrane and stored in the refrigerator below 4 Celsius prior to the tests. The remaining mixture was separated into AGS and

water through a filter screen, and the separated AGS was washed 3 times with tap water to remove residual Na_2CO_3 due to its adverse effect on AGS which can be known from Chapter 2. Then, after absorbing moisture through the filter paper, the AGS was returned to the original reactor.

3.2.5 Effect of dynamic adsorption/desorption process on AGS

Three SBR reactors were used to study the effect of dynamic adsorption/desorption process on AGS, named R0, Rc and Rd-50-1. R0 is the blank control group, that is, the ordinary SBR operating mode without Cr (VI) addition. Rc is the control group, that is, 5 mg/L Cr (VI) was added to the influent without desorption. Rd-50-1, namely 50% AGS was used for desorption at 1 time/d, was the experimental group; or the influent contained 5 mg/L Cr (VI) and 50% AGS was taken out for 1 time at a fixed time (14:00) every day after desorption and then returned to the original reactor.

3.2.6 Effect of different desorption ratios on AGS

Three desorption ratios, i.e. 25%, 50% and 75% were examined to investigate the effect of different desorption ratios on AGS, namely, Rd-25-1, Rd-50-1 and Rd-75-1, respectively. The desorption frequency for the above three SBRs was 1 time/d.

3.2.7 Effect of different desorption frequencies on AGS

Two desorption frequencies, i.e. 1 time/d (namely Rd-50-1) and 1time/2 d (namely Rd-50-2) were used to investigate the effect of different desorption frequencies on AGS. The desorption ratio of the above two SBRs was 50%. The main operating parameters of each reactor are listed in Table 3-1.

3.2.8 Analytical methods

NH_4^+-N, nitrous nitrogen (NO_2^--N), nitrate nitrogen (NO_3^--N) and phosphate (PO_4^{3-}-P) were determined by Liquid Chromatography (Shimadzu, Japan). A single AGS was placed in a graduated cylinder filled with 2 L of water, and the time required to fall from a fixed height of 42.3 cm was used to determine the settling velocity. The average value resulted from 100 randomly sampled AGS was used for each SBR in this study. The determination of the other parameters was the same as described in section 2.2.6.

3.3 Results and discussion

3.3.1 Effects of dynamic adsorption/desorption process on Cr (VI) removal and desorption by AGS

The effect of different desorption frequencies on Cr (VI) removal by AGS is shown in Fig. 3-1a. As seen, the Cr (VI) removal in the reactor (Rc) without dynamic adsorption/desorption obtained the highest cumulative Cr (VI) removal (2.11 mg) than the other two reactors. And a lower desorption frequency (1 time/2d) showed a better Cr (VI) removal performance. That is, a higher desorption frequency is not conducive to the Cr (VI) removal by AGS as desorption process may adversely affect the adsorption sites on the AGS. Also, the effects of different AGS desorbed biomass proportion on the Cr (VI) removal by AGS was investigated as shown in Fig. 3-1b. No significant difference was noticed between the three reactors in terms of Cr (VI) removal. But for the cumulative desorbed Cr (VI), the desorption ratios exhibited a significant effect among the three reactors (Fig. 3-1c). The higher the biomass desorption ratio, the higher the cumulative desorbed Cr (VI). Therefore, a higher biomass desorption ratio and desorption frequency are beneficial for the cumulative desorption of Cr (VI) while with an adverse effect on the removal of Cr (VI).

3.3.2 Effects of dynamic adsorption/desorption process on contaminant removal by AGS

Figs. 3-2a, b and c show the effects of dynamic adsorption/desorption process on ammonia nitrogen (NH_4^+-N) removal by AGS. As can be seen from Fig. 3-2a, at the same influent NH_4^+-N concentration (50 mg/L), the effluent NH_4^+-N concentration in the reactor without dynamic adsorption/desorption (Rc) increased quickly from day 5 and maintained around 31 mg/L during days 20-35. This observation may be associated with the cumulative inhibitory effect and toxicity of Cr on the nitrifying bacteria in AGS. While the reactor with dynamic adsorption/desorption (Rd) also showed similar phenomenon in the first 5 days, and the effluent NH_4^+-N concentration kept increase slightly till day 13; however, after that day it decreased to 16.69 mg/L. It can be seen that the increase in the effluent NH_4^+-N concentration with dynamic adsorption/desorption (Rd) is much earlier than that of control reactor (Rc), which is due to the double effects of the toxic inhibition of Cr (VI) and the adverse effect of dynamic adsorption/desorption on AGS. After a period of adaptation (days 5-13), desorption operation seemed to mitigate the inhibitory effect of Cr on ammonia nitrogen nitrification as the effluent NH_4^+-N

concentration decreased from day 13. The inhibition of Cr (VI) on the nitrification was completely eliminated during days 25-31. Possibly due to the above-mentioned double effects of dynamic adsorption/desorption process and Cr on AGS, the nitrification ability of AGS deteriorated again. The blank reactor (R0) exhibited a stable NH_4^+-N removal efficiency (averagely 99.67%).

Fig. 3-2b shows the effect of different desorbed biomass proportion on the NH_4^+-N removal by AGS. All of the reactors demonstrated the same trends, except that an earlier inhibition of nitrification appeared in the reactor with a higher desorption ratio, which may be related to the layer structure of bacteria in AGS where nitrifying bacteria are always located in the out layer. However, they also showed a mitigating effect on Cr inhibition of nitrification as the effluent NH_4^+-N concentrations from the three reactors decreased after day 13. And a higher biomass desorption ratio is beneficial to prolong the time for eliminating the inhibition effect of Cr (VI) on nitrification. On the other hand, no significant difference was observed between the two kinds of desorption frequency, except that the time for eliminating the inhibition effect of Cr (VI) on nitrification was longer at a higher desorption frequency (Fig. 3-2c).

Figs. 3-3a, b and c show the variations of effluent NO_2^--N concentrations from the different reactors. As can be seen from Fig. 3-3a, almost no NO_2^--N in the effluent was detected in the reactor without desorption (Rc), possibly due to the nitrification was inhibited by Cr (VI). While the effluent NO_2^--N increased as the inhibition of nitrification by Cr (VI) was reduced because of dynamic adsorption/desorption, and decreased due to the double effects of toxic inhibition of Cr (VI) and dynamic adsorption/desorption on AGS. As for different desorbed biomass proportions, the effluent NO_2^--N from the reactor with 25% and 75% desorbed biomass proportions were much higher than that from the reactor with 50% biomass desorption ratio, which may be associated with the balance between the mitigation of inhibitory effect of Cr by desorption and the adverse effect of desorption itself on AGS. Being similar with NH_4^+-N, the difference in effluent NO_2^--N between the two kinds of desorption frequency can be ignored (Fig. 3-3c). The blank group (R0) exhibited stable nitrification performance without little NO_2^--N accumulation observed.

Figs. 3-4a, b and c show the variations of effluent NO_3^--N from different reactors. As can be seen from Fig. 3-4a, the effluent NO_3^--N from R0 was around 29.15 mg/L, which reflected a downward trend possibly due to improved denitrification. While for the other two reactors, the effluent NO_3^--N concentration decreased, and this phenomenon appeared earlier in Rd, possibly due to the double effects of toxic inhibition of Cr (VI)

and the adverse impact of desorption on AGS. Fig. 3-4b shows that the decrease of effluent NO_3^--N concentration occurred earlier in the reactor with a high biomass desorption ratio, which corresponds to the increase of NH_4^+-N and NO_2^--N in Fig.3-2b and Fig.3-3b, respectively. Seen from Fig. 3-4c, the two kinds of desorption frequency show no significant difference on the variation of effluent NO_3^--N concentration, which is similar with effluent NH_4^+-N. Therefore, dynamic adsorption/desorption process can reduce the inhibition effect of Cr (VI) on AGS nitrification. From the results of the tested scenarios, the influence of desorption ratio is greater than that of desorption frequency.

Figs. 3-5a, b and c summarize the changes of effluent PO_4^{3-}-P from the three reactors. Fig. 3-5a shows that the effluent PO_4^{3-}-P reached the maximum on day 3 in Rd, which is much higher and earlier than that from Rc with only Cr (VI) addition. But after that the effluent PO_4^{3-}-P decreased quickly and kept at a lower concentration than that from Rc, probably due to the adaptation of AGS to the adsorption/desorption operation strategy and the alleviation of Cr(V) inhibition by desorption on P removal by AGS. Fig. 3-5b shows that the effluent PO_4^{3-}-P from the three reactors with different desorbed biomass proportions exhibited the similar trend with the maximum effluent PO_4^{3-}-P concentration increased with the increase of biomass desorption ratio. There is no significant difference between the two different desorption frequencies except the difference in the occurrence time of the maximum PO_4^{3-}-P concentration (Fig. 3-5c). Therefore, dynamic adsorption/desorption operation can also mitigate Cr (VI) inhibition on PO_4^{3-}-P removal by AGS. Among the tested scenarios, the biomass desorption ratio showed a greater influence on PO_4^{3-}-P removal than the desorption frequency.

Figs. 3-6a, b and c reflect the variations of effluent COD from the three reactors. Seen from Fig. 3-6a, the effluent COD from R0 had the lowest COD values, showing the best COD removal efficiency (98.89%). The effluent COD from Rd increased first and then decreased after day 3, possibly because AGS needs some time to adapt to the dynamic adsorption/desorption operation conditions. After this adaptation period, its effluent COD concentration was lower than that from Rc, especially during days 20-35. In addition, the reactors with different biomass desorption ratios showed the similar COD trend: The effluent COD decreased with the increase of biomass desorption ratio. Furthermore, there is no significant difference between the reactors with different desorption frequencies except that the effluent COD varied in a zigzag pattern at the desorption frequency of 1 time/2d. As for all the reactors operated under dynamic adsorption/desorption, the effluent COD showed a downward trend, indicating that AGS can adapt to dynamic adsorption/desorption and behave better in pollutants removal.

Overall, a higher biomass desorption ratio and desorption frequency is conducive to the COD removal by AGS under dynamic adsorption/desorption.

3.3.3 Effects of dynamic adsorption/desorption process on biochemical characteristics of AGS.

In this study, specific oxygen uptake rate (SOUR) was introduced to represent the bioactivity of AGS. Figs. 3-7a, b and c show the changes of SOUR of AGS in the three reactors. Seen from Fig. 3-7a, an increased trend was observed in the SOUR of AGS in R0 along with its operation. The lowest SOUR of AGS was detected in Rc due to the toxicity of Cr (VI) on microorganism. The SOUR of AGS in Rd decreased in the first 5 days, most probably due to the double effects from the toxic inhibition of chromium and the adverse impact of desorption on AGS; after that the SOUR increased, which may be resulted from the adaption of AGS to the dynamic adsorption/desorption operation and increase in specific surface area due to granule breakage. Figs. 3-7b and c indicate that the effects of different biomass desorption ratios and desorption frequencies on SOUR are not significant.

Figs. 3-8a, b and c demonstrate the changes of EPS in AGS from the three reactors. It can be seen from Fig. 3-8a that Cr (VI) addition and dynamic adsorption/desorption have insignificant effect on PS secretion but have negative effect on PN contents in AGS. It was found that lower biomass desorption ratio and desorption frequency are beneficial to maintain the amount of PN in AGS, which is not observed on the amount of PS.

Integrity coefficient was applied to characterize the stability of AGS. Figs. 3-9a, b and c show the variations of integrity coefficient of AGS in the three reactors. Seen from Fig. 3-9a, compared to R0, dynamic adsorption/desorption operation may exert adverse effect on AGS stability, while the addition of Cr (VI) seems to be beneficial to maintain the stability of AGS, possibly due to the inhibition effect of Cr (VI) on the growth of filamentous bacteria. Also, Figs. 3-9b and c indicate that a lower biomass desorption ratio is conducive to maintain the stability of AGS in SBR under the dynamic adsorption/desorption operation, and different desorption frequency didn’t show significant effect on the stability of AGS.

Settling velocity is one of the important indicators for AGS settleability. The settling velocities of AGS from the three reactors are shown in Figs. 3-10a, b and c. No significant difference was observed among the results from different biomass desorption ratio and desorption frequency (Figs. 3-10a, b and c). All the settling velocities of AGS for all the reactors decreased from 30.82 to 15.74 m/h, which mainly due to the average size of AGS

decreased from 1.10 to 0.42 mm (Fig. 3-11a, b and c). As shown in Fig. 3-11a, b and c, all the MLVSS in different reactors decreased quickly in the first 5 days from 4.47 to 2.97 g/L except that in Rc, and then decreased slowly, which means that the low concentration of Cr (5 mg/L) is beneficial to maintain the MLVSS of AGS. However, the long-term addition of low-concentration Cr will cause the SVI of AGS to increase, which is not conducive to the sedimentation of sludge (Fig. 3-12a). Also, dynamic adsorption/desorption operation will cause SVI to rise sharply in the first 5 days, but after AGS was adapted to dynamic adsorption/desorption operation, SVI gradually decreased, which is lower than that of Rc and higher than that of R0 (Fig. 3-12a). A higher biomass desorption ratio will result in a higher SVI in the first 5 days, but after that, there is no obvious difference (Fig. 3-12b). The peak of SVI with lower desorption frequency (1time/2d) will appear later than that with higher desorption frequency (1time/d). After that, there is no significant difference between the two reactors (Fig. 3-12c).

3.4 Summary

In this chapter, the effects of dynamic adsorption/desorption on AGS were investigated under different operation conditions. Results show that a higher biomass desorption ratio and desorption frequency are beneficial to the cumulative desorption mass of Cr (VI) while have an adverse effect on the removal of Cr (VI). Throughout the experiment, Cr (VI) exhibited inhibition on nitrification and PO_4^{3-}-P removal. In the latter period of the experiment, dynamic adsorption/desorption operation reflected mitigation effect on Cr inhibition of nitrification and PO_4^{3-}-P removal. However, the long-term double effects from the adverse impact of Cr (VI) toxicity suppression and desorption on AGS make the nitrification and phosphorus removal performance of AGS eventually deteriorate. Desorbed biomass proportion rather than different desorption frequency may have noticeable effects on the mitigation of Cr (VI) inhibition of nitrification. However, no significant difference in the mitigation of PO_4^{3-}-P removal was observed among test desorbed biomass proportions and desorption frequencies. In addition, a higher biomass desorption ratio and desorption frequency is conducive to COD removal by AGS under dynamic adsorption/desorption. Furthermore, dynamic adsorption/desorption is beneficial to maintain the bioactivity of AGS but not conducive to the stability and settleability of AGS and maintenance of PN in EPS. In any case, the deterioration of stability and settleability is still within the acceptable levels. Thus dynamic adsorption/desorption may be proposed as a promising option to mitigate the negative impact of Cr (VI) on AGS.

Table 3-1. List of main operating parameters of each reactor

Reactors	R0	Rc	Rd-25-1	Rd-50-1	Rd-75-1	Rd-50-2
Influent Cr (VI) (mg/L)	0	5	5	5	5	5
Desorption ratio (%)	--	--	25	50	75	50
Desorption frequency	--	--	1 time/d	1 time/d	1 time/d	1 time/2d

(a)

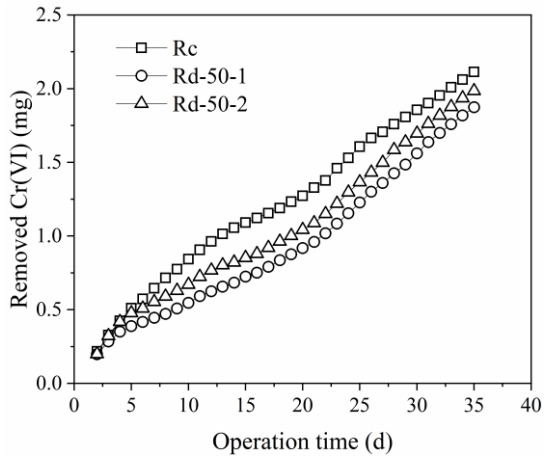

(b)

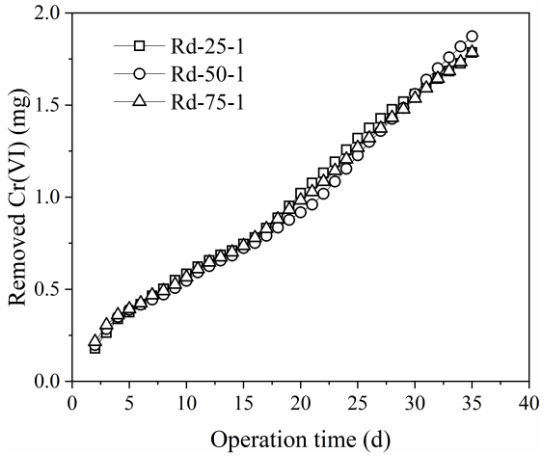

(c)

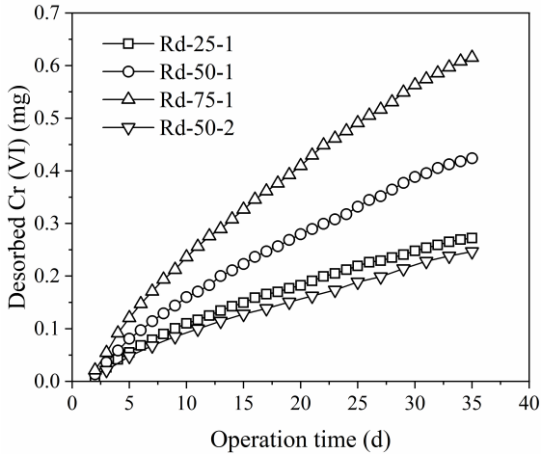

Fig. 3-1. Effects of different desorption frequencies (a), and desorbed biomass proportion (b) on Cr (VI) removal. And effects of different desorption frequency and desorbed biomass proportion on desorbed Cr (VI) (c).

(a)

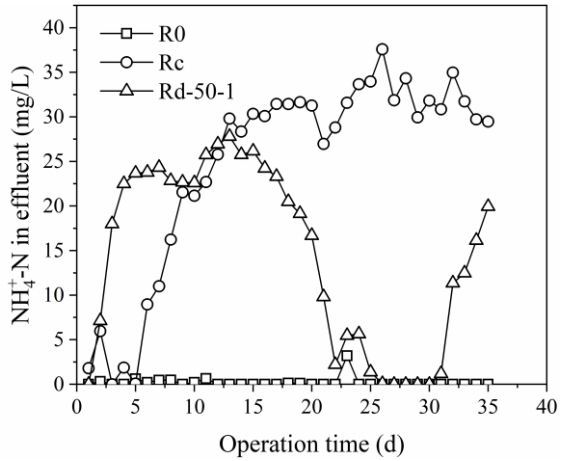

(b)

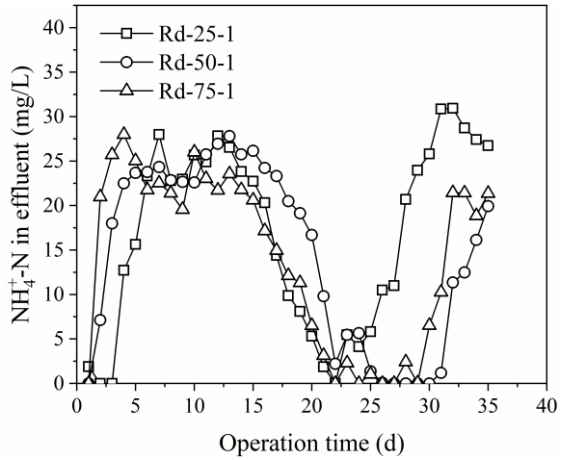

(c)

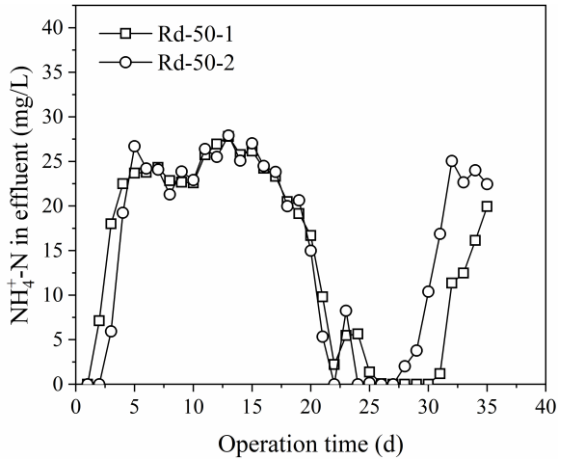

Fig. 3-2. Comparison of NH_4^+-N removal between reactors with/without dynamic adsorption/desorption (a), and effects of desorbed biomass proportion (b) and different desorption frequency (c) on NH_4^+-N removal.

(a)

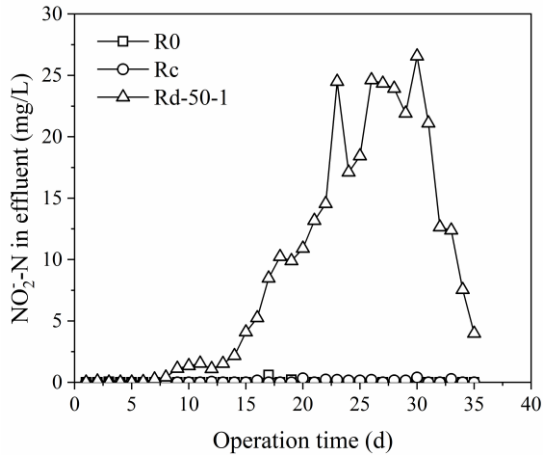

(b)

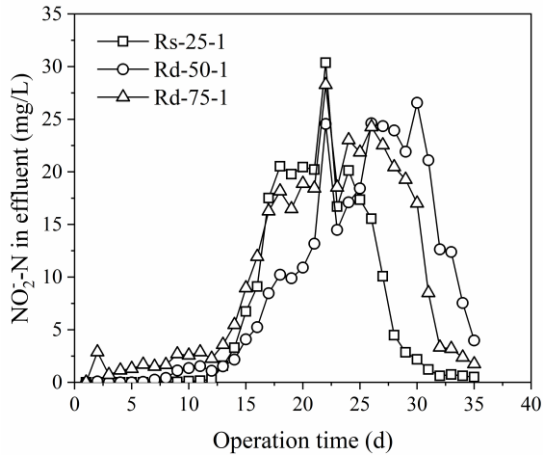

(c)

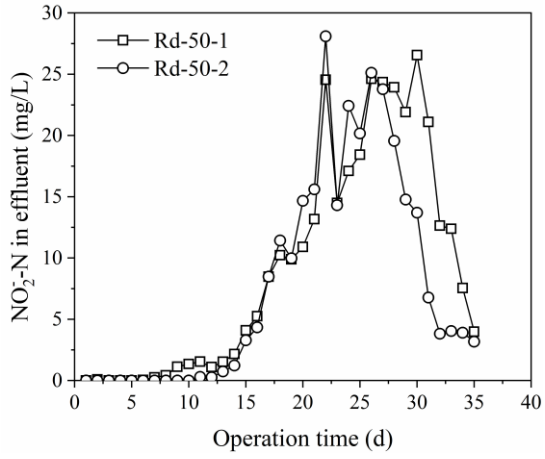

Fig. 3-3. Comparison of effluent NO_2^--N in the reactors with and without dynamic adsorption/desorption (a). And effects of desorbed biomass proportion (b) and different desorption frequency (c) on effluent NO_2^--N concentration.

(a)

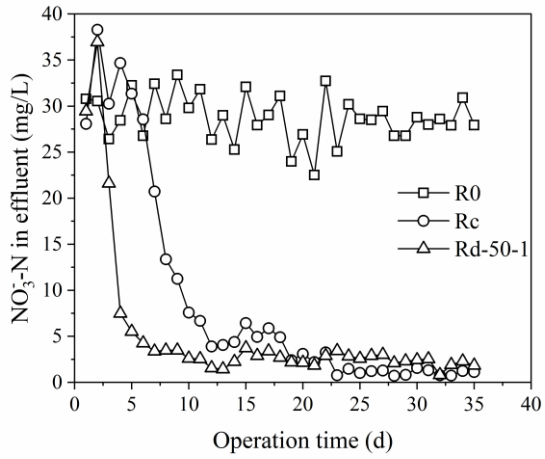

(b)

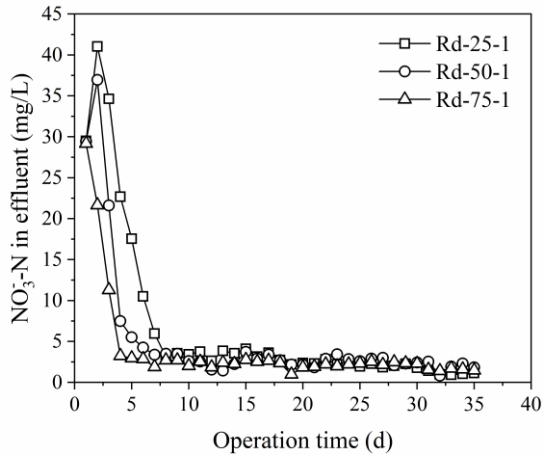

(c)

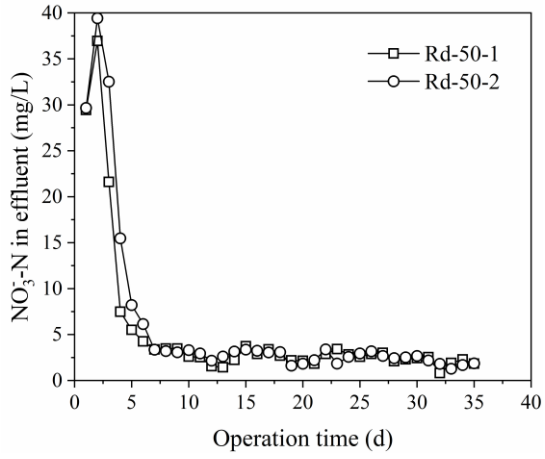

Fig. 3-4. Comparison of effluent NO_3^--N in the reactors with and without dynamic adsorption/desorption (a). And effects of desorbed biomass proportion (b) and different desorption frequency (c) on effluent NO_3^--N concentration.

(a)

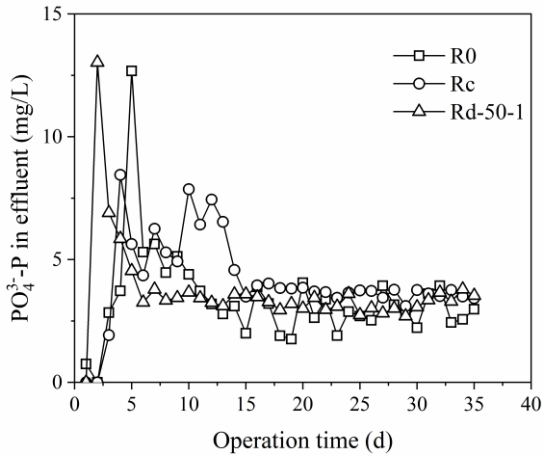

(b)

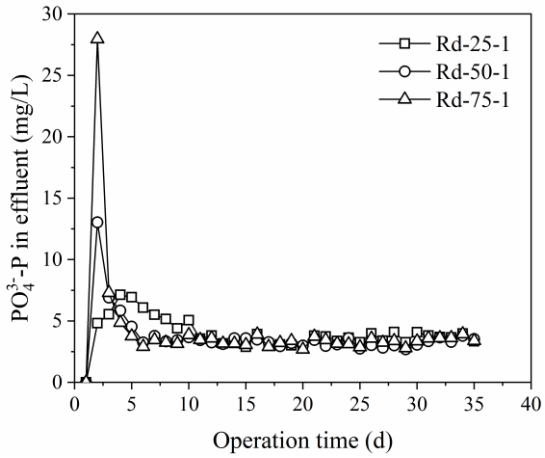

(c)

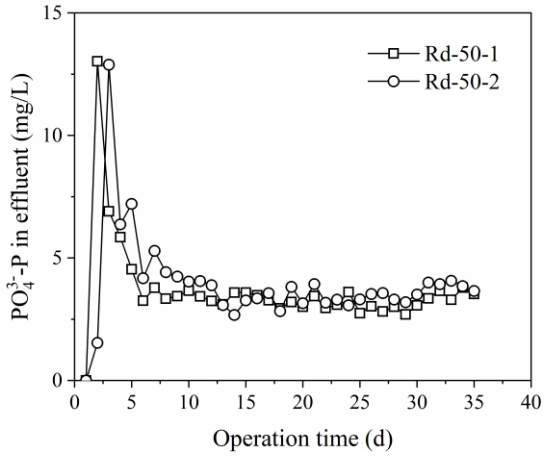

Fig. 3-5. Comparison of effluent PO_4^{3-}-P in the reactors with and without dynamic adsorption/desorption (a). And effects of desorbed biomass proportion (b) and different desorption frequency (c) on effluent PO_4^{3-}-P concentration.

(a)

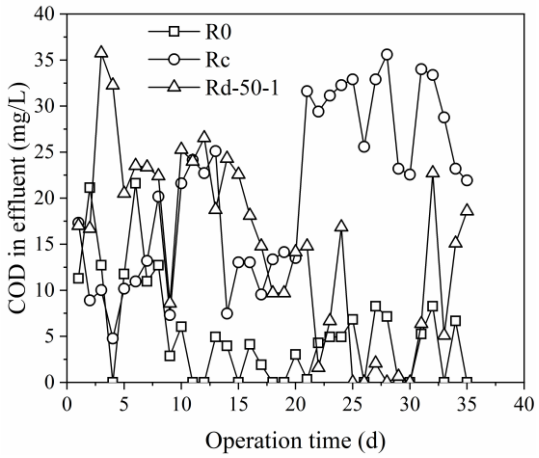

(b)

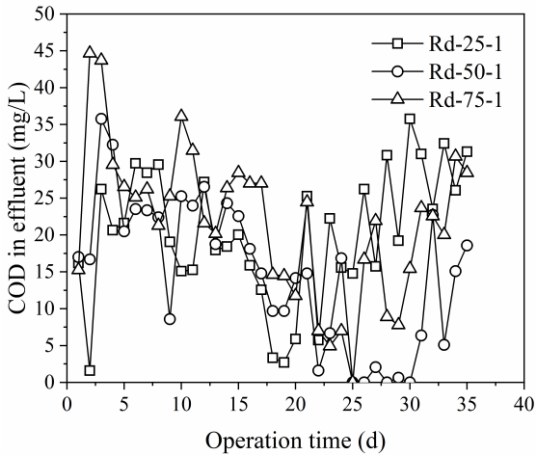

(c)

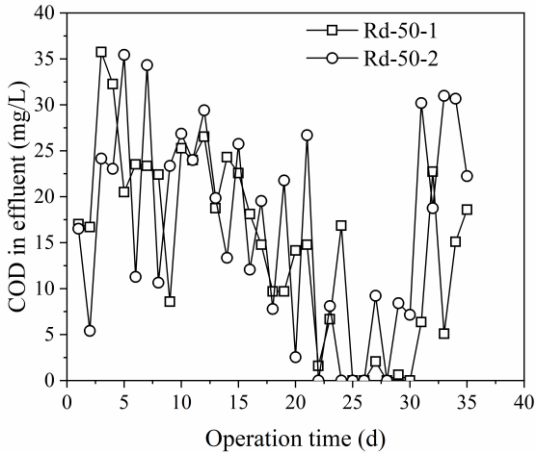

Fig. 3-6. Comparison of effluent COD in reactors with and without dynamic adsorption/desorption (a). And effects of desorbed biomass proportion (b) and different desorption frequency (c) on effluent COD concentration.

(a)

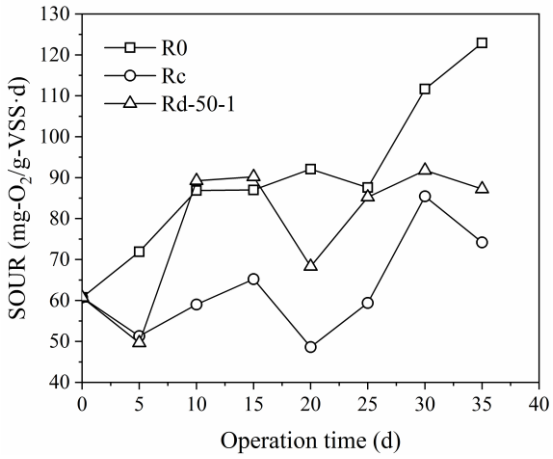

(b)

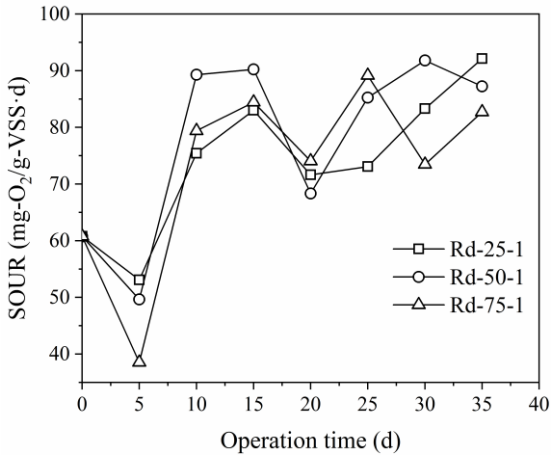

(c)

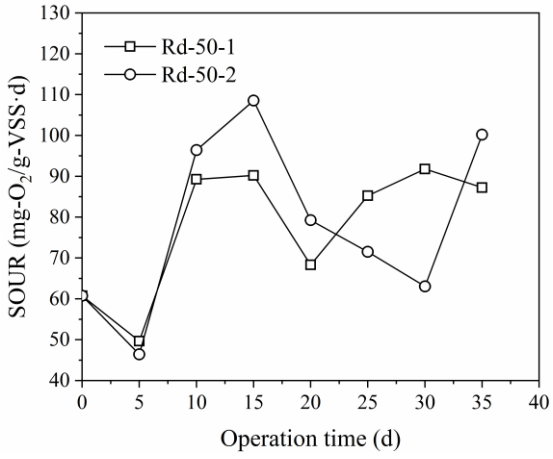

Fig. 3-7. Comparison of SOUR of AGS in reactors with and without dynamic adsorption/desorption (a). And effects of desorbed biomass proportion (b) and different desorption frequency (c) on the granular SOUR.

(a)

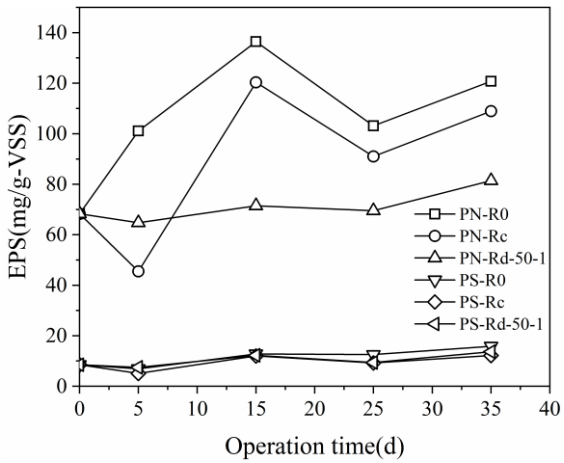

(b)

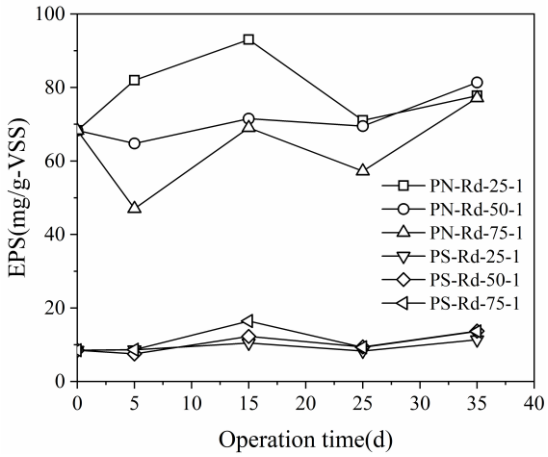

(c)

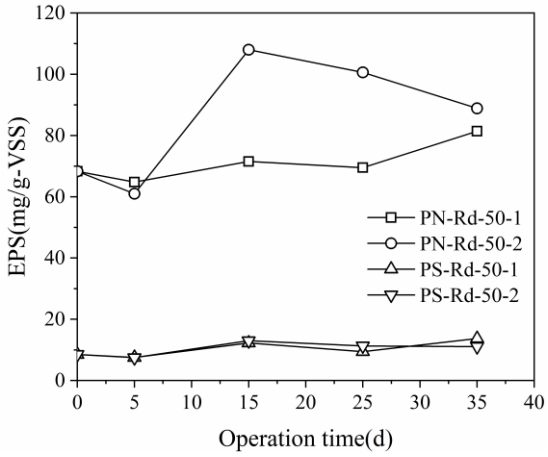

Fig. 3-8. Comparison of EPS content in AGS from reactors with and without dynamic adsorption/desorption (a). And effects of desorbed biomass proportion (b) and different desorption frequency (c) on EPS content.

(a)

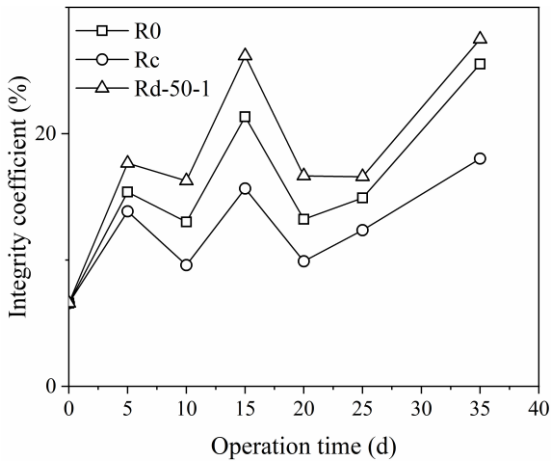

(b)

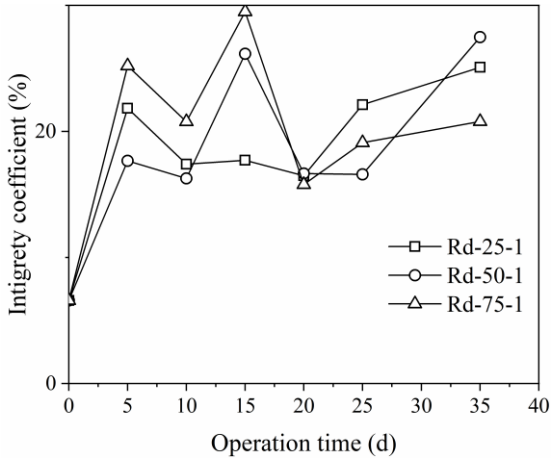

(c)

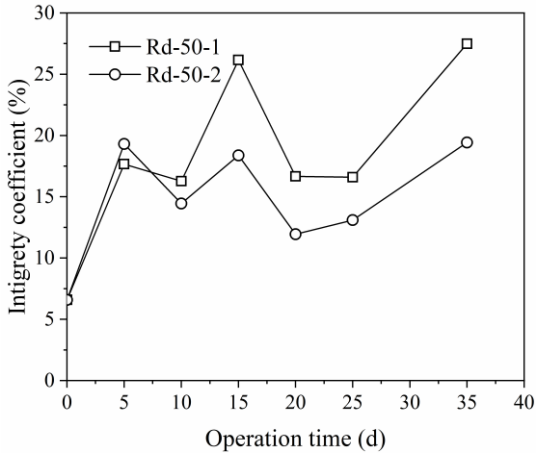

Fig. 3-9. Comparison of integrity coefficient of AGS from reactors with and without dynamic adsorption/desorption (a). And effects of desorbed biomass proportion (b) and different desorption frequency(c) on integrity coefficient of AGS.

(a)

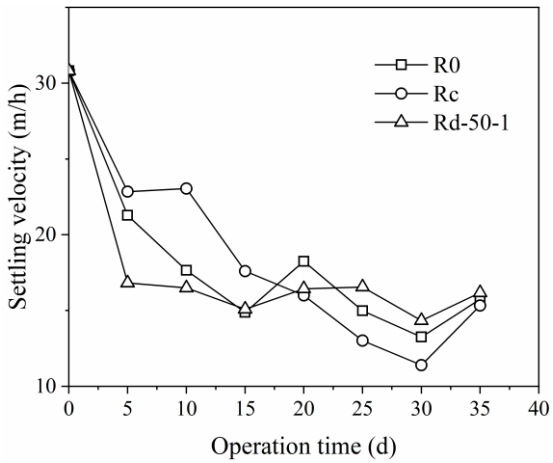

(b)

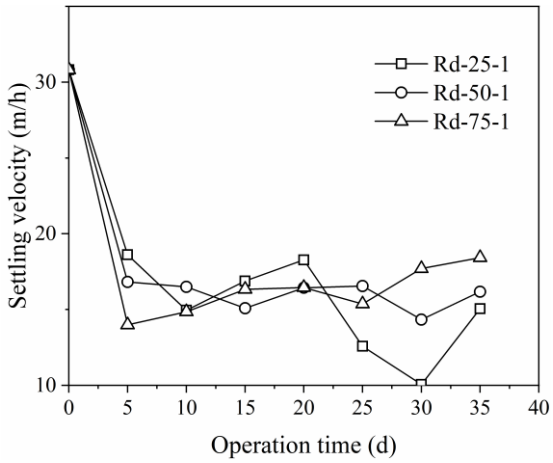

(c)

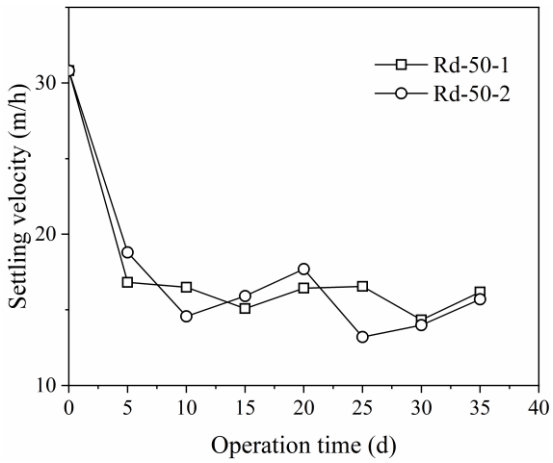

Fig. 3-10. Comparison of settling velocity of AGS from reactors with and without dynamic adsorption/desorption (a). And effects of desorbed biomass proportion (b) and different desorption frequency (c) on settling velocity of AGS.

(a)

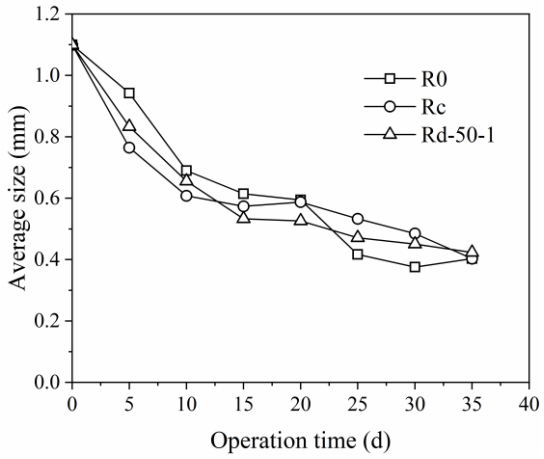

(b)

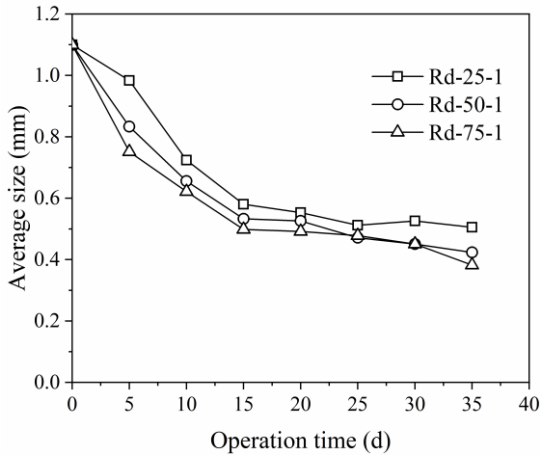

(c)

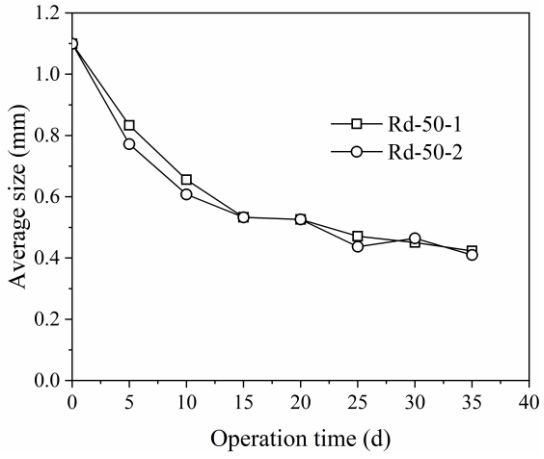

Fig. 3-11. Comparison of average size of AGS from reactors with and without dynamic adsorption/desorption (a). And effects of desorbed biomass proportion (b) and different desorption frequency (c) on average size of AGS.

(a)

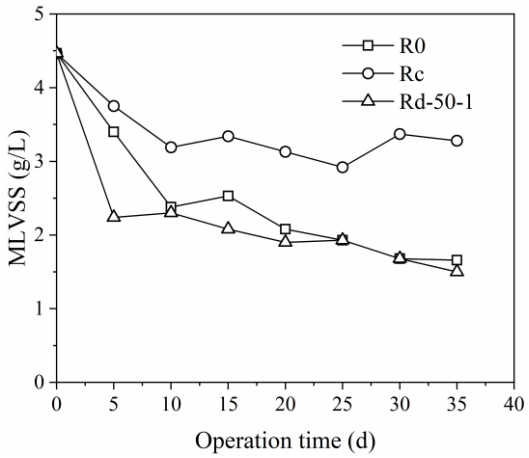

(b)

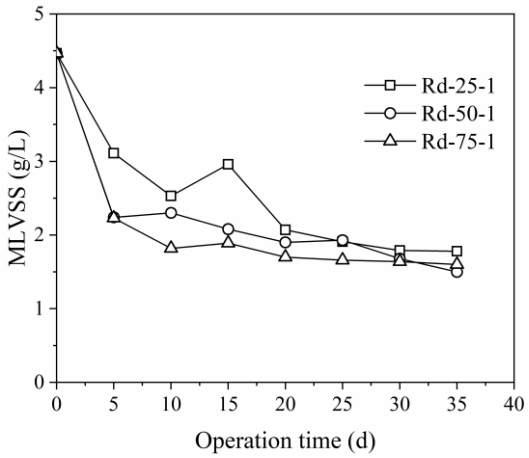

(c)

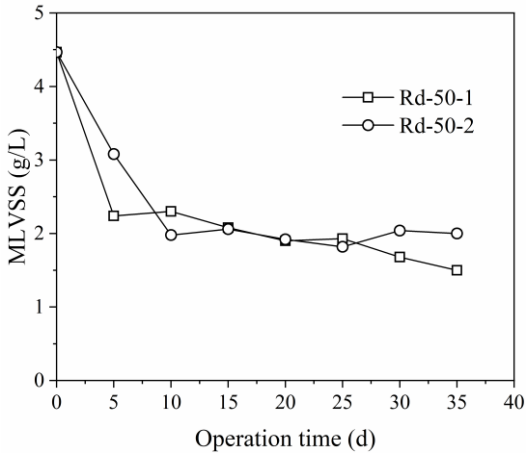

Fig. 3-12. Comparison of MLVSS of AGS from reactors with and without dynamic adsorption/desorption (a). And effects of desorbed biomass proportion (b) and different desorption frequency (c) on MLVSS of AGS.

(a)

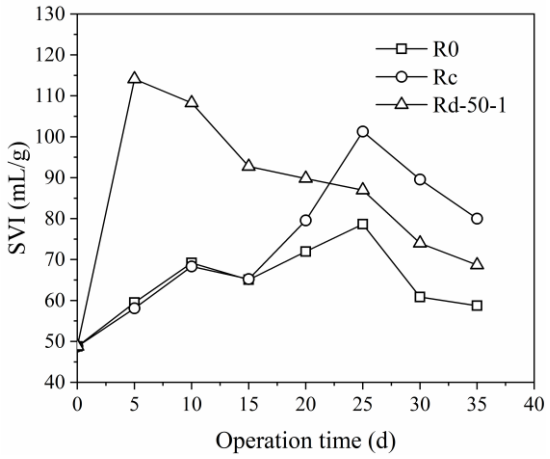

(b)

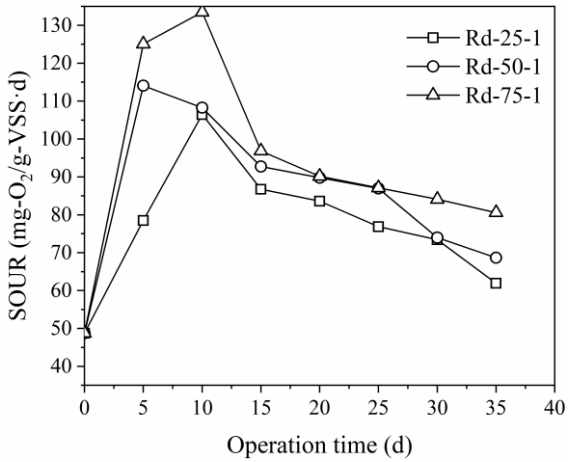

(c)

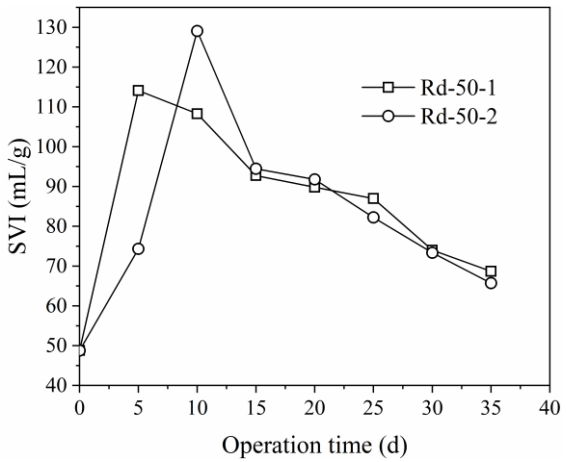

Fig. 3-13. Comparison of SVI of AGS from reactors with and without dynamic adsorption/desorption (a). And effects of desorbed biomass proportion (b) and different desorption frequency (c) on SVI of AGS.

Chapter 4 Effect of OLR on AGS performance during the operation of dynamic Cr (VI) adsorption/desorption

4.1 Introduction

In Chapter 3, the reactor performance under dynamic adsorption/desorption operation show its superiority to the reactor without dynamic adsorption/desorption in terms of COD, NH_4^+-N and PO_4^{3-}-P removal. Although dynamic adsorption/desorption is beneficial to maintain the bioactivity of AGS, it`s not conducive to the stability and settleability of AGS. So in this chapter, the focus is directed to the stability and settleability of AGS due to the operation of dynamic adsorption/desorption. OLR is regarded as one of the important operating parameters that affect the performance of AGS systems during dynamic adsorption/desorption process. In this study, three different OLRs (0.5, 1, 2 kg COD/m^3·d) at a desorption frequency of 1 time/d were used to explore its effect on the stability of AGS.

4.2 Materials and methods

4.2.1 Synthetic wastewater and AGS

The composition of the synthetic wastewater was same as in section 2.2.2 except the Cr (VI) and COD concentration. In this chapter, the initial Cr (VI) concentration was 5 mg/L. and COD was 250, 500, 1000 mg/L for the three reactors (I, II, and III), resulting in OLR of 0.5, 1, 2 kg COD/m^3·d, respectively. The AGS was also sampled from the same 1L SBR in the laboratory, which has been cultivated for more than two years as described in Chapters 2 and 3. The initial sludge concentration was set as 5 g-MLSS/L.

4.2.2 Reactor set-up

This study was carried out using three identical laboratory scale column plexiglass sequencing batch reactors with a working volume of 250 mL each as described in Section 3.2.2. Except the OLR condition, the operating parameters of the reactors were the same as in Section 3.2.2.

4.2.3 Experimental procedure

The three identical reactors were used for this study, which were operated at OLR of

0.5, 1, 2 kg COD/m^3·d, respectively, with an initial Cr (VI) concentration of 5 mg/L. After every two cycles of operation, half of the AGS in each reactor was taken out for once desorption with 0.5 M Na_2CO_3 as the desorbent under 45℃ due to that the high temperature is conducive to the desorption of Cr (VI). The desorption experiments were conducted in 250 mL Erlenmeyer flasks containing Cr-loaded AGS and 100 mL desorption solution each. Then the mixture was shaken at 125 rpm at room temperature for 60 min. After desorption, the AGS was washed three times with tap water and then returned to the original reactor to continue the subsequent cycles of operation.

4.2.4 Analytical methods

Parameters including mixed liquor (volatile) suspended solids (ML(V)SS) were determined according to the standard methods (APHA, 2012). Morphology of granules samples of the granules were qualitatively observed using Leica M205 C Microscope (Leica Microsystems, Switzerland). The determination of the remaining parameters is the same as in Section 2.2.6 and 3.2.8.

4.3 Results and discussion

4.3.1 Adsorption and desorption of Cr (VI) on AGS

The reactors with different OLR 0.5, 1 and 2 kg COD/m^3·d were labelled as Reactor I, II and III, respectively. The AGS system with adsorption/desorption model was run for 30 cycles to investigate the effect of different OLR on the AGS. Fig. 4-1 shows the variation of Cr (VI) removal efficiency under the designed OLRs. It can be seen that in the first 6 cycle the Cr (VI) removal efficiency by Reactor I, II, and III decreased quickly from 71.78, 73.31 and 74.35% to 8.46, 8.97and 9.39%, respectively; and then kept at an average Cr (VI) removal efficiency of 3.73, 5.04 and 7.05% reflecting an overall slow downward trend till the 30^{th} cycle, respectively. This observation indicates that the AGS system has limited capability to continuously treat Cr (VI)-containing wastewater, which may be due to the limited adsorption sites possessed by a certain quantity of AGS. When the adsorption sites reach saturation, the adsorption removal of Cr (VI) by the AGS system reaches its upper limit. It was noted that the Cr (VI) removal efficiency at OLR of 2 kg COD/m^3·d was higher than those of 0.5 and 1kg COD/m^3·d, meaning that a higher OLR is beneficial for Cr (VI) removal during the dynamic adsorption/desorption AGS system. This phenomenon may be contributed by the increased microbial activity under a higher OLR which can help the microbes survive the tough and toxic conditions.

Furthermore, in the cycle after desorption from the 6th to 30th cycles, the removal efficiency of Cr (VI) has been slightly improved attributable to the desorption, with an average increase of 0.85, 0.93, 0.98% at 0.5, 1, and 2 kg COD/m^3·d, respectively. This further proves that a higher OLR is beneficial to Cr (VI) removal by AGS system under dynamic adsorption/desorption.

Figs. 4-2a and b show the cumulative amount of removed Cr (VI) and desorbed Cr (VI) under the test OLRs. Reactor III at 2 kg COD/m^3·d showed the highest cumulative amount of removed Cr (VI) and desorbed Cr (VI), about 2.15 mg and 0.46 mg Cr (VI) respectively, which are apparently higher than those by the other two reactors at lower OLRs. It thus is confirmed that a higher OLR is conducive to Cr (VI) adsorption and desorption in the AGS system.

4.3.2 Changes in physical and chemical properties of AGS

The SOUR and integrity coefficient were also introduced to characterize the bioactivity and stability of AGS. The variations of SOUR and integrity coefficient of AGS in the three reactors are illustrated in Figs. 4-3a and b. It can be seen that as for the AGS in the three reactors, the SOUR decreased and the integrity coefficient increased as the experiment progressed. The SOUR decreased from initial 10.96 to 1.82, 2.79 and 5.46 for the AGS in Reactors I, II and III, respectively; and the integrity coefficient increased from initial 6.00% to 57.69, 25.61 and 21.85%, respectively. Among them, Reactor III showed the best performance with a smaller decrease in SOUR and a smaller increase in integrity coefficient. This indicates that a higher OLR (2 kg COD/m^3·d) favors the maintenance of biological activity and granular stability in comparison to lower OLR conditions (≦1 kg COD/m^3·d).

Figs. 4-4a and b show that the MLVSS concentrations in the three reactors decreased from around 2.6 g/L to 1.1, 1.2 and 1.5 g/L, which is mainly due to AGS breakage during the operation as its strength became weak, which were easy to be discharged from the system along with the effluent. The MLVSS concentration can also be predicted from the increased integrity coefficient of AGS.

On the other hand, seen from Figs. 4-5a and b, the decrease in average particle size and settling velocity proved that the granules were broken. The average size of AGS decreased from 1.02 mm to 0.52, 0.60 and 0.71 mm, and their average settling velocity decreased from 22.79 m/h to 7.81, 10.19 and 11.57 m/h for the granules in Reactors I, II and III, respectively. Compared to other parameters, the extent of reduction in average granule size was relatively small, because the broken pellets were easily washed out from

the system through effluent discharge, while the remaining ones were relatively large ones. The average settling velocity decreased by > 50% for the three reactors, most probably due to repeated adsorption/desorption operations which generally loosen the granular structure, no matter small or large ones. Further work is necessary on the improvement of granular structure during dynamic adsorption/desorption operation.

The morphological changes of AGS during the adsorption/desorption process also evidenced the above viewpoint. From Figs. 4-6, the original AGS on day 0 has a tight structure with a smooth and regular surface. While the morphology of AGS changed a lot as the structure turned looser with rougher granular surface along with the operation of the three reactors, even the granules in Reactor I experienced breakage and lost their stable inner core.

To sum up, during the repeated adsorption/desorption, all the indices relating to granular sludge properties got deteriorated, including SOUR, integrity coefficient, MLVSS, settling velocity, size and morphology, especially at the low OLR. At the same time, it can also be seen that high OLR is beneficial for AGS to maintain its physiochemical properties to cope with a toxic and tough living conditions, like repeated adsorption/desorption operations.

4.5 summary

In this chapter, the adsorption/desorption model was introduced to AGS system for Cr (VI) remove and recovery under different OLRs. The results show that a higher OLR can obtain a higher amount of Cr (VI) adsorption and desorption by the AGS system. A higher OLR helps AGS maintain the stability of its physical and chemical properties to overcome the negative effects from the toxic and tough conditions, like frequently adsorption/desorption operation. Results from this chapter indicate that increasing OLR may be a rescue strategy to maintain the stability of AGS system when Cr (VI) removal is targeted during dynamic adsorption/desorption.

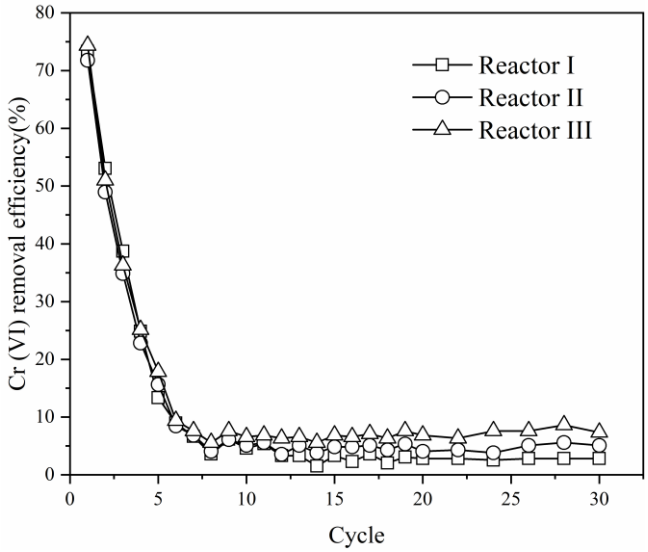

Fig. 4-1. Variation of Cr (VI) removal efficiency in AGS-SBR operated at different OLRs. (Influent Cr (VI) = 5 mg/L, OLRs for Reactors I, II and III are 0.5, 1, 2 kg COD/m^3·d, respectively)

(a)

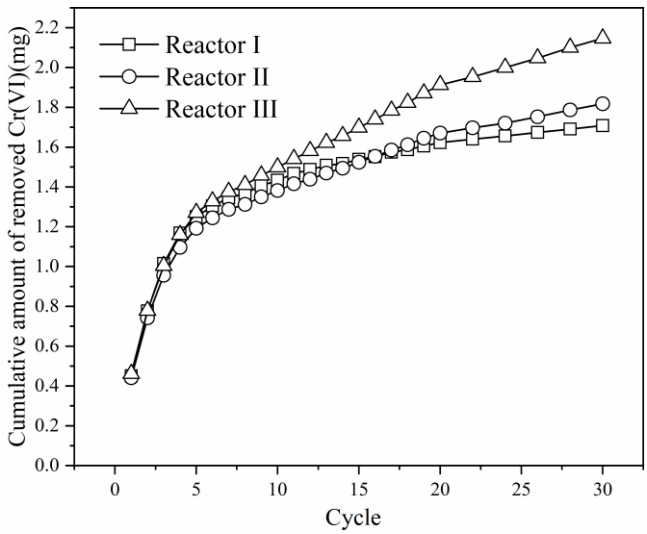

(b)

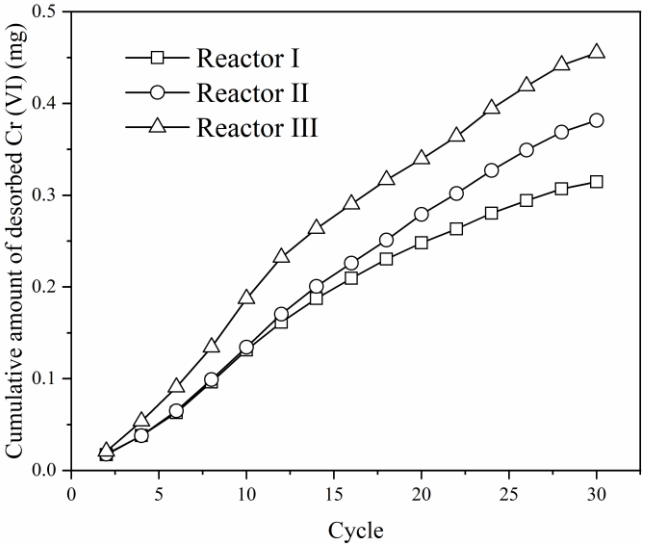

Fig. 4-2. Cumulative amount of removed Cr (VI) (a) and desorbed Cr (VI) (b) by AGS in three reactors operated at different OLRs. (Influent Cr (VI) = 5 mg/L, OLRs for Reactors I, II and III are 0.5, 1, 2 kg COD/m^3·d, respectively)

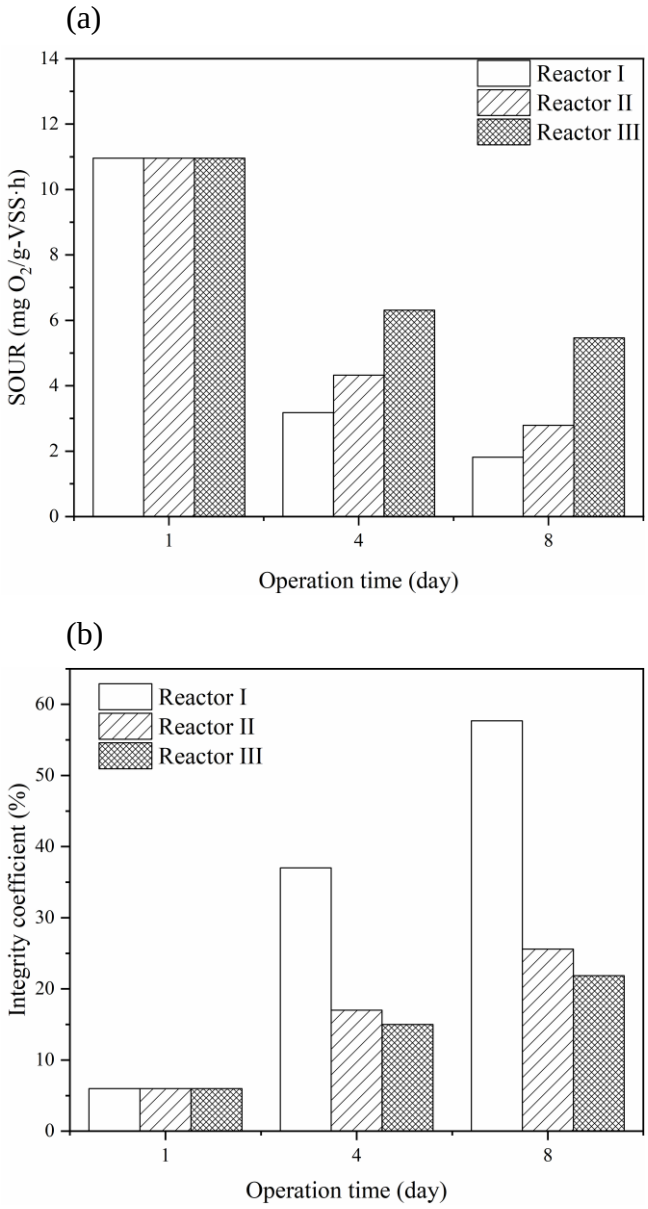

Fig. 4-3. Changes of SOUR (a) and integrity coefficient (b) of AGS in three reactor operated at different OLRs. (Influent Cr (VI) = 5 mg/L, OLRs for Reactors I, II and III are 0.5, 1, 2 kg COD/m^3·d, respectively)

(a)

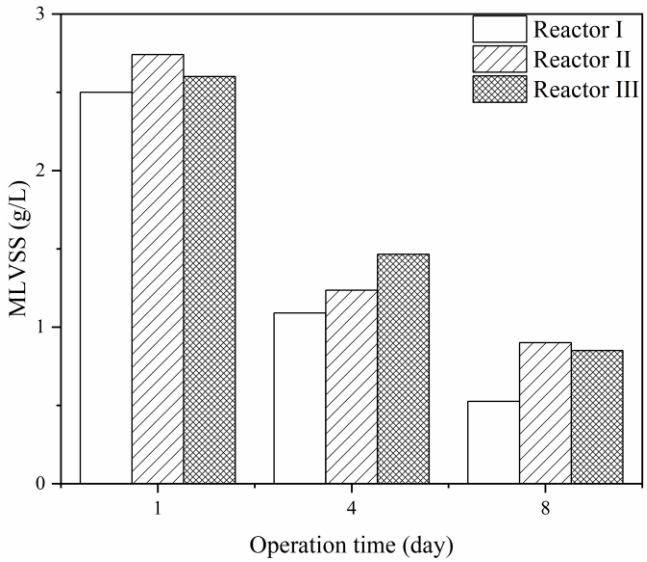

(b)

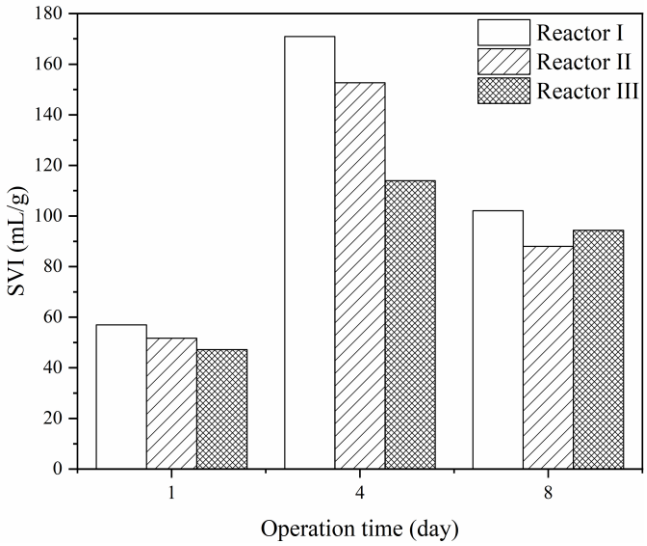

Fig. 4-4. Variation of MLVSS (a) and SVI (b) of AGS in three reactors operated at different OLRs. (Influent Cr (VI) = 5 mg/L, OLRs for Reactors I, II and III are 0.5, 1, 2 kg COD/m^3·d, respectively)

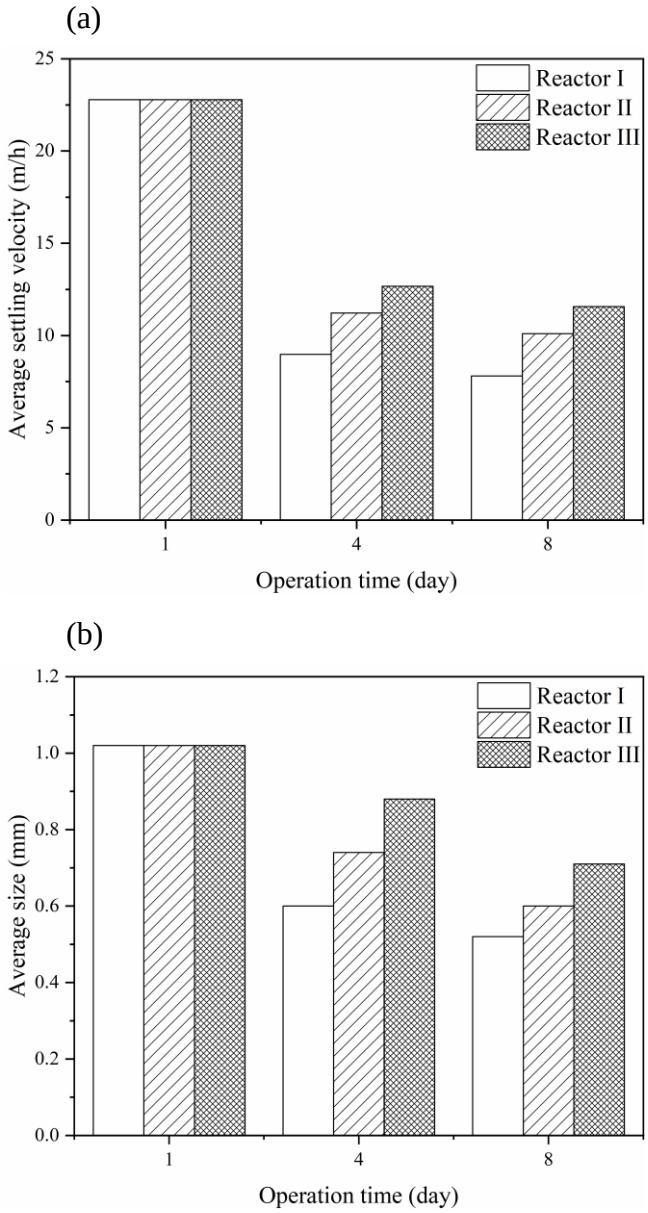

Fig. 4-5. Changes of average settling velocity (a) and size (b) of AGS in three reactors operated at different OLRs. (Influent Cr (VI) = 5 mg/L, OLRs for Reactors I, II and III are 0.5, 1, 2 kg COD/m^3·d, respectively)

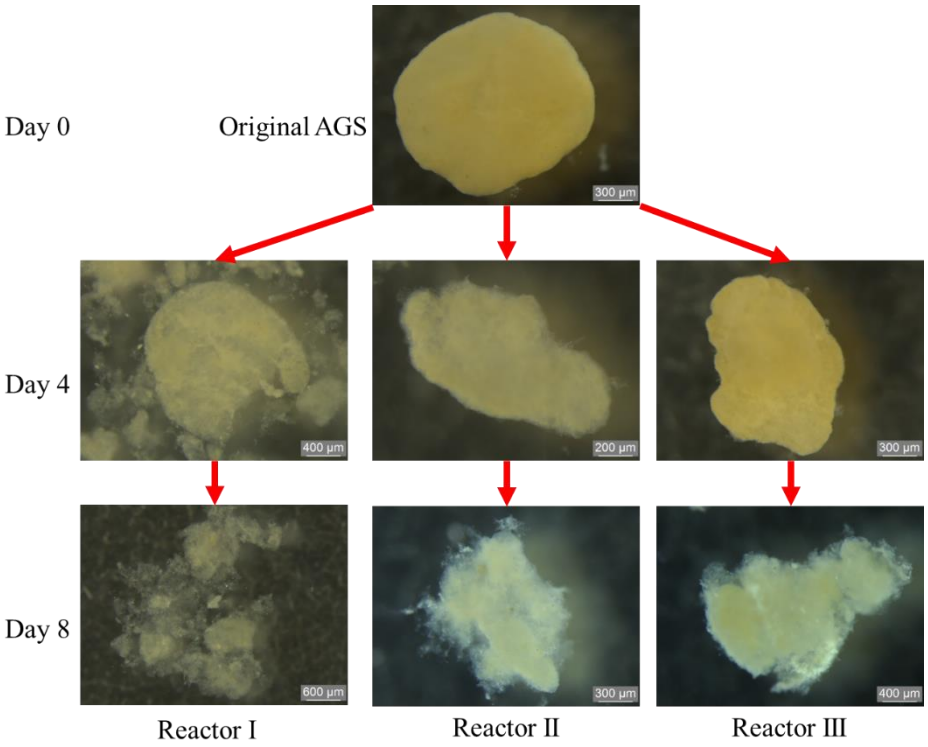

Fig. 4-6. Morphology changes of AGS in three reactors operated at different OLRs. (Influent Cr (VI) = 5 mg/L, OLRs for Reactors I, II and III are 0.5, 1, 2 kg COD/m^3·d, respectively)

Chapter 5 Conclusions and future research

5.1 Conclusions

Heavy metals removal and recovery from wastewater may challenge the sustainable operation of current WWTPs with activated sludge as the main treatment process. AGS originated from activated sludge can have more potentials for treating toxic heavy metals containing wastewater. This study attempted a novel operation strategy on AGS for Cr (VI) removal by introducing a dynamic adsorption/desorption process into the AGS system.

In the present study, five different desorbent solutions were tested for Cr (VI) desorption from Cr-loaded AGS. The effects of operation parameters on the granular bioactivity and stability of AGS were investigated. Two kinetic models were used to fit the desorption data. In addition, dynamic adsorption/desorption process was introduced into the AGS system, and its effects were examined on the AGS performance and granular properties under different conditions regarding the physicochemical and biological characteristics of AGS. The results from this study can be summarized as follows.

5.1.1 Main influencing factors during dynamic Cr (VI) adsorption/desorption operation of AGS system

(1) Desorbent selection and optimization of desorption condition

Cr (VI) adsorption onto active aerobic granular sludge (AGS) under neutral condition was explored and then focused on Cr (VI) desorption from the Cr-loaded AGS. The changes of AGS bioactivity and stability were also analyzed with respect to cations release and extracellular polymeric substances (EPS). Among the 6 test desorbents, Na_2CO_3 showed the best performance for Cr (VI) desorption from Cr-loaded AGS, reflecting a better fit to the pseudo-second-order kinetic model (R^2 = 0.985-0.995). Granular specific oxygen uptake rate (SOUR) was detected to decrease from the initial 22.38 to 5.55 mg-O_2/g-VSS·h after 60 min desorption by 1M Na_2CO_3, with integrity coefficient increased from 5.52% to 25.63%. Release of Ca^{2+}, Mg^{2+} and K^+ was mainly from EPS, especially the tightly bound EPS during the desorption process. Moreover, proteins rather than polysaccharides were found to be more sensitive to the increasing Na_2CO_3 concentration during the desorption process.

(2) Desorbed biomass proportion and desorption frequency

A higher desorbed biomass ratio and desorption frequency are beneficial to the cumulative desorption of Cr (VI) while with an adverse effect on the removal of Cr (VI). Different biomass desorption ratio shows a greater effect on the mitigation of Cr (VI) inhibition on nitrification than different desorption frequency in this study. But there is no significant difference between different biomass desorption ratio and different desorption frequency for mitigation of Cr (VI) inhibition on PO_4^{3-}-P removal. In addition, a higher biomass desorption ratio and desorption frequency is conducive to the COD removal by AGS under dynamic adsorption/desorption. Furthermore, dynamic adsorption/desorption is beneficial to maintain the bioactivity of AGS but not conducive to the stability and settleability of AGS and maintenance of PN. In any case, the deterioration of stability and settleability is still within acceptable limits.

(3) OLR

The effect of different OLRs on the removal and recovery of Cr (VI) and the physicochemical characters of AGS was investigated in the AGS system under the operation strategy of dynamic adsorption/desorption. The AGS system with a higher OLR (2 kg COD/m^3·day) can obtain a higher amount of Cr (VI) adsorption and desorption in the AGS system. The higher OLR (2 kg COD/m^3·day) is beneficial to maintain the stability of AGS physical and chemical properties in the toxic and frequent adsorption/desorption AGS systems.

5.1.2 Implications of this study

Throughout the experiment without dynamic adsorption/desorption, Cr (VI) exhibited inhibition on nitrification and PO_4^{3-}-P removal. In the latter part of the operation of AGS systems treating Cr (VI)-containing wastewater, the dynamic adsorption/desorption operation showed some mitigation effect on Cr (VI) inhibition of nitrification and PO_4^{3-}-P removal. And the higher OLR (2 kg COD/m^3·day) is beneficial to maintain the stability of AGS physical and chemical properties. This shows that dynamic adsorption/desorption process with high OLR can be used as an alternative strategy for the treatment of wastewater containing toxic and hazardous heavy metals through relieving their negative impact on AGS in the short term.

5.2 Future research

In order to promote the application of adsorption-desorption mode in the actual AGS-SBR system, future works should be conducted mainly from the following three aspects.

The first important work is to select and optimize the desorption solution, and its desorption condition. The desorption solution should satisfy the maximum desorption of heavy metals adsorbed by AGS without negative impact on the biological activity and stability of AGS.

The second step is to strengthen AGS by modification to ensure that AGS can maintain its stably biochemical functions in the treatment of toxic wastewater under repeated adsorption and desorption operation mode.

The third aspect is how to quickly regain AGS bioactivities when negative effects occur after the adsorption and desorption operation before returning to the AGS system. Some bioactive substances might be used to quickly ameliorate and restore AGS bioactivities if being negatively impacted by the dynamic adsorption and desorption operation.

References

Adav, S.S., Chen, M.Y., Lee, D.J., Ren, N.Q. 2007. Degradation of phenol by aerobic granules and isolated yeast Candida tropicalis. *Biotechnol. Bioeng.*, **96**(5), 844-52.

Adav, S.S., Lee, D.-J., Show, K.-Y., Tay, J.-H. 2008. Aerobic granular sludge: Recent advances. *Biotechnol. Adv.*, **26**(5), 411-423.

Addour, L., Belhocine, D., Boudries, N., Comeau, Y., Pauss, A., Mameri, N. 1999. Zinc uptake by Streptomyces rimosus biomass using a packed-bed column. *J. Chem. Technol. Biotechnol.*, **74**(11), 1089-1095.

Alloway, B.J. 2013. Introduction. in: *Heavy Metals in Soils: Trace Metals and Metalloids in Soils and their Bioavailability*, (Ed.) B.J. Alloway, Springer Netherlands. Dordrecht, pp. 3-9.

Anuar, A.N., Halim, M.H.A., Rosman, N.H., Othman, I., Harun, H., Basri, H.F., Ujang, Z., van Loosdrecht, M. 2020. Microbial identification and extracellular polymeric substances characterization of aerobic granules developed in treating rubber processing wastewater. in: *Valorisation of agro-industrial residues – Volume I: Biological approaches*, (Eds.) Z.A. Zakaria, R. Boopathy, J.R. Dib, Springer International Publishing. Cham, pp. 257-286.

Anyanwu, B.O., Ezejiofor, A.N., Igweze, Z.N., Orisakwe, O.E. 2018. Heavy metal mixture exposure and effects in developing nations: An update. *Toxics*, **6**(4).

APHA, 2012. Standard methods for the examination of water and wastewater, 22nd edition. American Public Health Association (APHA), American Water Works Association (AWWA) and Water Environment Federation (WEF), Washington, D.C., USA.

Aqeel, H., Weissbrodt, D.G., Cerruti, M., Wolfaardt, G.M., Wilén, B.-M., Liss, S.N. 2019. Drivers of bioaggregation from flocs to biofilms and granular sludge. *Environ. Sci.-Wat. Res.*, **5**(12), 2072-2089.

Barr, J.J., Cook, A.E., Bond, P.L. 2010a. Granule formation mechanisms within an aerobic wastewater system for phosphorus removal. *Appl. Environ. Microbiol.*, **76**(22), 7588-97.

Barr, J.J., Slater, F.R., Fukushima, T., Bond, P.L. 2010b. Evidence for bacteriophage activity causing community and performance changes in a phosphorus-removal activated sludge. *FEMS Microbiol. Ecol.*, **74**(3), 631-42.

Basuvaraj, M., Fein, J., Liss, S.N. 2015. Protein and polysaccharide content of tightly and loosely bound extracellular polymeric substances and the development of a

granular activated sludge floc. *Water Res.*, **82**, 104-117.

Beun, J.J., Heijnen, J.J., van Loosdrecht, M.C. 2001. N-removal in a granular sludge sequencing batch airlift reactor. *Biotechnol. Bioeng.*, **75**(1), 82-92.

Beun, J.J., Hendriks, A., van Loosdrecht, M.C.M., Morgenroth, E., Wilderer, P.A., Heijnen, J.J. 1999. Aerobic granulation in a sequencing batch reactor. *Water Res.*, **33**(10), 2283-2290.

Bradford, M.M. 1976. A rapid and sensitive method for the quantitation of microgram quantities of protein utilizing the principle of protein-dye binding. *Anal. Biochem.*, **72**(1), 248-254.

Cai, W., Jin, M., Zhao, Z., Lei, Z., Zhang, Z., Adachi, Y., Lee, D.-J. 2018. Influence of ferrous iron dosing strategy on aerobic granulation of activated sludge and bioavailability of phosphorus accumulated in granules. *Bioresour. Technol. Rep.*, 2, 7-14.

Cao, Y., Zhang, S., Wang, G., Li, T., Xu, X., Deng, O., Zhang, Y., Pu, Y. 2017. Enhancing the soil heavy metals removal efficiency by adding HPMA and PBTCA along with plant washing agents. *J. Hazard. Mater.*, **339**, 33-42.

Carucci, A., Milia, S., De Gioannis, G., Piredda, M. 2009. Acetate-fed aerobic granular sludge for the degradation of 4-chlorophenol. *J. Hazard. Mater.*, **166**(1), 483-490.

Cassidy, D.P., Belia, E. 2005. Nitrogen and phosphorus removal from an abattoir wastewater in a SBR with aerobic granular sludge. *Water Res.*, **39**(19), 4817-4823.

Chaturvedi, A.D., Pal, D., Penta, S., Kumar, A. 2015. Ecotoxic heavy metals transformation by bacteria and fungi in aquatic ecosystem. *World J. Microb. Biot.*, 31(10), 1595-1603.

Chen, K., Zhao, Z., Yang, X., Lei, Z., Zhang, Z., Zhang, S. 2018. Desorption trials and granular stability of chromium loaded aerobic granular sludge from synthetic domestic wastewater treatment. *Bioresour. Technol. Rep.*, **1**, 9-15.

Chung, T.-P., Tseng, H.-Y., Juang, R.-S. 2003. Mass transfer effect and intermediate detection for phenol degradation in immobilized *Pseudomonas putida* systems. *Process Biochem.*, **38**(10), 1497-1507.

Coma, M., Verawaty, M., Pijuan, M., Yuan, Z., Bond, P.L. 2012. Enhancing aerobic granulation for biological nutrient removal from domestic wastewater. *Bioresour. Technol.*, **103**(1), 101-108.

Cossich, E.S., da Silva, E.A., Tavares, C.R.G., Filho, L.C., Ravagnani, T.M.K. 2004. Biosorption of chromium(III) by biomass of Seaweed *Sargassum* sp. in a fixed-bed column. *Adsorption*, **10**(2), 129-138.

Daneshvar, E., Vazirzadeh, A., Niazi, A., Kousha, M., Naushad, M., Bhatnagar, A. 2017. Desorption of Methylene blue dye from brown macroalga: Effects of operating parameters, isotherm study and kinetic modeling. *J. Clean. Prod.*, **152**, 443-453.

Deng, S., Wang, L., Su, H. 2016. Role and influence of extracellular polymeric substances on the preparation of aerobic granular sludge. *J. Environ. Manage.*, **173**, 49-54.

Dhal, B., Thatoi, H.N., Das, N.N., Pandey, B.D. 2013. Chemical and microbial remediation of hexavalent chromium from contaminated soil and mining/metallurgical solid waste: A review. *J. Hazard. Mater.*, **250-251**, 272-291.

DuBois, M., Gilles, K.A., Hamilton, J.K., Rebers, P.A., Smith, F. 1956. Colorimetric method for determination of sugars and related substances. *Anal. Chem.*, **28**(3), 350-356.

Duque, A.F., Bessa, V.S., Carvalho, M.F., de Kreuk, M.K., van Loosdrecht, M.C.M., Castro, P.M.L. 2011. 2-Fluorophenol degradation by aerobic granular sludge in a sequencing batch reactor. *Water Res.*, **45**(20), 6745-6752.

Emamverdian, A., Ding, Y., Mokhberdoran, F., Xie, Y. 2015. Heavy metal stress and some mechanisms of plant defense response. *Sci. World J.*, **2015**, 756120.

Fang, H.H.P., Xu, L.-C., Chan, K.-Y. 2002. Effects of toxic metals and chemicals on biofilm and biocorrosion. *Water Res.*, **36**(19), 4709-4716.

Fang, J., Su, B., Sun, P., Lou, J., Han, J. 2015. Long-term effect of low concentration Cr (VI) on P removal in granule-based enhanced biological phosphorus removal (EBPR) system. *Chemosphere*, **121**, 76-83.

Ghangrekar, M.M., Asolekar, S.R., Joshi, S.G. 2005. Characteristics of sludge developed under different loading conditions during UASB reactor start-up and granulation. *Water Res.*, **39**(6), 1123-1133.

Guo, W., Ngo, H.-H., Li, J. 2012. A mini-review on membrane fouling. *Bioresour. Technol.*, **122**, 27-34.

Gupta, V.K., Rastogi, A. 2008. Sorption and desorption studies of chromium(VI) from nonviable cyanobacterium *Nostoc muscorum* biomass. *J. Hazard. Mater.*, **154**(1), 347-354.

Habibul, N., Hu, Y., Wang, Y.-K., Chen, W., Yu, H.-Q., Sheng, G.-P. 2016. Bioelectrochemical chromium(VI) removal in plant-microbial fuel cells. *Environ. Sci. Technol.*, **50**(7), 3882-3889.

Hamiruddin, N., Awang, N., Shaaban, M. 2019. The performance of extracellular polymeric substance (EPS) on stability of aerobic granular sludge (AGS). C*iv.*

Environ. Eng. Rep., 29(3), 60.

He, Q., Chen, L., Zhang, S., Wang, L., Liang, J., Xia, W., Wang, H., Zhou, J. 2018. Simultaneous nitrification, denitrification and phosphorus removal in aerobic granular sequencing batch reactors with high aeration intensity: Impact of aeration time. *Bioresour. Technol.*, **263**, 214-222.

Higgins Matthew, J., Novak John, T. 1997. Characterization of exocellular protein and its role in bioflocculation. *J. Environ. Eng.*, **123**(5), 479-485.

Jayakumar, R., Rajasimman, M., Karthikeyan, C. 2015. Sorption and desorption of hexavalent chromium using a novel brown marine algae *Sargassum myriocystum*. *Korean J. Chem. Eng.*, **32**(10), 2031-2046.

Jiang, H.L., Tay, J.H., Liu, Y., Tay, S.T. 2003. Ca^{2+} augmentation for enhancement of aerobically grown microbial granules in sludge blanket reactors. *Biotechnol. Lett.*, **25**(2), 95-9.

Jiang, H.-L., Tay, J.-H., Maszenan, A.M., Tay, S.T.-L. 2004. Bacterial diversity and function of aerobic granules engineered in a sequencing batch reactor for phenol degradation. *Appl. Environ. Microbiol*, **70**(11), 6767-6775.

Jobby, R., Jha, P., Yadav, A.K., Desai, N. 2018. Biosorption and biotransformation of hexavalent chromium [Cr (VI)]: A comprehensive review. *Chemosphere*, **207**, 255-266.

Kamaludeen, S.P.B., Megharaj, M., Juhasz, A.L., Sethunathan, N., Naidu, R. 2003. Chromium-microorganism interactions in soils: Remediation implications. in: *Reviews of Environmental Contamination and Toxicology*, (Ed.) G.W. Ware, Springer New York. New York, NY, pp. 93-164.

Kamble, S.M. 2014. Water pollution and public health issues in Kolhapur city in Maharashtra. *Int. J. Sci. Res. Publ.*, **4**(1), 1-6.

Kanojia, R.K., Junaid, M., Murthy, R.C. 1998. Embryo and fetotoxicity of hexavalent chromium: a long-term study. *Toxicol. Lett.*, **95**(3), 165-72.

Khan, M. A. and Ghouri, A. M., 2011. Environmental pollution: Its effects on life and its remedies. *Res. World J. Arts Sci. Comm.*, 2(2), 276-285.

Khan, M.Z., Mondal, P.K., Sabir, S. 2013. Aerobic granulation for wastewater bioremediation: A review. *Can. J. Chem. Eng.*, **91**(6), 1045-1058.

Khosravi, R., Moussavi, G., Ghaneian, M.T., Ehrampoush, M.H., Barikbin, B., Ebrahimi, A.A., Sharifzadeh, G. 2018. Chromium adsorption from aqueous solution using novel green nanocomposite: Adsorbent characterization, isotherm, kinetic and thermodynamic investigation. *J. Mol. Liq.*, **256**, 163-174.

Kiran Kumar Reddy, G., Nancharaiah, Y.V. 2018. Sustainable bioreduction of toxic levels of chromate in a denitrifying granular sludge reactor. *Environ. Sci. Pollut. Res.*, **25**(2), 1969-1979.

Knez, Ž., Škerget, M., KnezHrnčič, M. 2013. 1 - Principles of supercritical fluid extraction and applications in the food, beverage and nutraceutical industries. in: *Separation, Extraction and Concentration Processes in the Food, Beverage and Nutraceutical Industries*, (Ed.) S.S.H. Rizvi, Woodhead Publishing, pp. 3-38.

Kong, Q., Ngo, H.H., Shu, L., Fu, R.-s., Jiang, C.-h., Miao, M.-s. 2014. Enhancement of aerobic granulation by zero-valent iron in sequencing batch airlift reactor. *J. Hazard. Mater.*, **279**, 511-517.

Li, J., Feng, J., Yan, W. 2013. Excellent adsorption and desorption characteristics of polypyrrole/TiO_2 composite for methylene blue. *Appl. Surf. Sci.*, **279**, 400-408.

Li, X.Y., Yang, S.F. 2007. Influence of loosely bound extracellular polymeric substances (EPS) on the flocculation, sedimentation and dewaterability of activated sludge. *Water Res.*, **41**(5), 1022-1030.

Li, Y., Liu, Y., Xu, H. 2008. Is sludge retention time a decisive factor for aerobic granulation in SBR? *Bioresour. Technol.*, **99**(16), 7672-7677.

Lidsky, T.I., Schneider, J.S. 2003. Lead neurotoxicity in children: basic mechanisms and clinical correlates. *Brain*, **126**(Pt 1), 5-19.

Liu, Q.S., Tay, J.H., Liu, Y. 2003a. Substrate concentration-independent aerobic granulation in sequential aerobic sludge blanket reactor. *Environ. Technol.*, **24**(10), 1235-1242.

Liu, W., Zhang, J., Jin, Y., Zhao, X., Cai, Z. 2015. Adsorption of Pb (II), Cd (II) and Zn (II) by extracellular polymeric substances extracted from aerobic granular sludge: Efficiency of protein. *J. Environ. Chem. Eng.*, **3**(2), 1223-1232.

Liu, X.-M., Sheng, G.-P., Yu, H.-Q. 2007. DLVO approach to the flocculability of a photosynthetic H_2-producing bacterium, *Rhodopseudomonas acidophila*. *Environ. Sci. Technol.*, **41**(13), 4620-4625.

Liu, X.-W., Sheng, G.-P., Yu, H.-Q. 2009. Physicochemical characteristics of microbial granules. *Biotechnol. Adv.*, **27**(6), 1061-1070.

Liu, Y., Lam, M.C., Fang, H.H. 2001. Adsorption of heavy metals by EPS of activated sludge. *Water Sci. Technol.*, **43**(6), 59-66.

Liu, Y., Lin, Y.-M., Yang, S.-F., Tay, J.-H. 2003b. A balanced model for biofilms developed at different growth and detachment forces. *Process Biochem.*, **38**(12), 1761-1765.

Liu, Y., Tay, J.-H. 2004. State of the art of biogranulation technology for wastewater treatment. *Biotechnol. Adv.*, **22**(7), 533-563.

Liu, Y.-Q., Moy, B., Kong, Y.-H., Tay, J.-H. 2010. Formation, physical characteristics and microbial community structure of aerobic granules in a pilot-scale sequencing batch reactor for real wastewater treatment. *Enzyme Microb. Technol.*, **46**(6), 520-525.

Lobos, J., Wisniewski, C., Heran, M., Grasmick, A. 2008. Sequencing versus continuous membrane bioreactors: Effect of substrate to biomass ratio (F/M) on process performance. *J. Membr. Sci.*, **317**(1), 71-77.

Losi, M.E., Amrhein, C., Frankenberger, W.T. 1994. Environmental Biochemistry of Chromium. in: *Reviews of Environmental Contamination and Toxicology*, (Ed.) G.W. Ware, Springer New York. New York, NY, pp. 91-121.

Lv, Y., Wan, C., Lee, D.-J., Liu, X., Tay, J.-H. 2014. Microbial communities of aerobic granules: Granulation mechanisms. *Bioresour. Technol.*, **169**, 344-351.

Mahmood, Q., Rashid, A., Ahmad, S.S., Azim, M.R., Bilal, M. 2012. Current Status of Toxic Metals Addition to Environment and Its Consequences. in: *The Plant Family Brassicaceae: Contribution Towards Phytoremediation*, (Eds.) N.A. Anjum, I. Ahmad, M.E. Pereira, A.C. Duarte, S. Umar, N.A. Khan, Springer Netherlands. Dordrecht, pp. 35-69.

Marsh, T.L., McInerney, M.J. 2001. Relationship of hydrogen bioavailability to chromate reduction in aquifer sediments. *Appl. Environ. Microbiol*, **67**(4), 1517-1521.

Mayer, C., Moritz, R., Kirschner, C., Borchard, W., Maibaum, R., Wingender, J., Flemming, H.-C. 1999. The role of intermolecular interactions: studies on model systems for bacterial biofilms. *Int. J. Biol. Macromol.*, **26**(1), 3-16.

McCarroll, N., Keshava, N., Chen, J., Akerman, G., Kligerman, A., Rinde, E. 2010. An evaluation of the mode of action framework for mutagenic carcinogens case study II: chromium (VI). *Environ. Mol. Mutagen.*, **51**(2), 89-111.

McSwain, B.S., Irvine, R.L., Hausner, M., Wilderer, P.A. 2005. Composition and distribution of extracellular polymeric substances in aerobic flocs and granular sludge. *Appl. Environ. Microbiol.*, **71**(2), 1051-1057.

Mehtab H., Muhammad F. M., Asma J., Sidra A., Nayab A., Sharon Z. and Jaweria H. 2017. Water pollution and human health. *Environ. Risk Asses. Remed.*, 1(3):16-19.

Moy, B.Y.-P., Tay, J.-H., Toh, S.-K., Liu, Y., Tay, S.T.-L. 2002a. High organic loading influences the physical characteristics of aerobic sludge granules. *Lett. Appl.*

Microbiol., **34**(6), 407-412.

Nakai, K., Yoneda, K., Nakagawa, T., Moriue, T., Kubota, Y. 2016. Phosphate buffered saline induces filaggrin expression in a human epidermal keratinocyte cell line (HaCaT cells). *J. Dermatol. Sci.*, **84**(1), e137.

Nancharaiah, Y.V., Dodge, C., Venugopalan, V.P., Narasimhan, S.V., Francis, A.J. 2010. Immobilization of Cr (VI) and its reduction to Cr(III) phosphate by granular biofilms comprising a mixture of microbes. *Appl. Environ. Microbiol.*, 76(8), 2433-8.

Nancharaiah, Y.V., Kiran Kumar Reddy, G. 2018. Aerobic granular sludge technology: Mechanisms of granulation and biotechnological applications. *Bioresour. Technol.*, **247**, 1128-1143.

Nancharaiah, Y.V., Venkata Mohan, S., Lens, P.N.L. 2016. Recent advances in nutrient removal and recovery in biological and bioelectrochemical systems. *Bioresour. Technol.*, **215**, 173-185.

Nancharaiah, Y.V., Venugopalan, V.P., Francis, A.J. 2012. Removal and biotransformation of U (VI) and Cr (VI) by aerobically grown mixed microbial granules. *Desalin. Water Treat.*, **38**(1-3), 90-95.

Ni, B.-J., Yu, H.-Q. 2010. Mathematical modeling of aerobic granular sludge: A review. *Biotechnol. Adv.*, 28(6), 895-909.

Oliveira, H. 2012. Chromium as an environmental pollutant: Insights on induced plant toxicity. *J. Bot.*, **2012**, 375843.

Otero, M., Cutillas-Barreiro, L., Nóvoa-Muñoz, J.C., Arias-Estévez, M., Fernández-Sanjurjo, M.J., Álvarez-Rodríguez, E., Núñez-Delgado, A. 2015. Cr (VI) sorption/desorption on untreated and mussel-shell-treated soil materials: fractionation and effects of pH and chromium concentration. *Solid Earth*, **6**(2), 373-382.

Ozdemir, G., Ceyhan, N., Ozturk, T., Akirmak, F., Cosar, T. 2004. Biosorption of chromium(VI), cadmium(II) and copper(II) by Pantoea sp. TEM18. *Chem. Eng. J.*, **102**(3), 249-253.

Pan, S., Tay, J.H., He, Y.X., Tay, S.T. 2004. The effect of hydraulic retention time on the stability of aerobically grown microbial granules. *Lett. Appl. Microbiol.*, **38**(2), 158-63.

Pandey, G., Sharma, M. 2014. Heavy metals causing toxicity in animals and fishes. *Res. J. Anim. Vet. Fish. Sci.*, **2**, 17-23.

Paul, D. 2017. Research on heavy metal pollution of river Ganga: A review. *Ann. Agrar.*

Sci., **15**(2), 278-286.

Qin, L., Liu, Y., Tay, J.-H. 2004. Effect of settling time on aerobic granulation in sequencing batch reactor. *BioChem. Eng. J.*, **21**(1), 47-52.

Quiton, K.G., Doma, B., Futalan, C.M., Wan, M.-W. 2018. Removal of chromium(VI) and zinc(II) from aqueous solution using kaolin-supported bacterial biofilms of Gram-negative E. coli and Gram-positive Staphylococcus epidermidis. *Sustain. Environ. Res.*, **28**(5), 206-213.

Rahman, Z., Singh, V.P. 2020. Bioremediation of toxic heavy metals (THMs) contaminated sites: concepts, applications and challenges. *Environ. Sci. Pollut. Res*., **27**, 27563–27581.

Rezaei, H. 2016. Biosorption of chromium by using *Spirulina* sp. *Arab. J. Chem.*, **9**(6), 846-853.

Saha, R., Nandi, R., Saha, B. 2011. Sources and toxicity of hexavalent chromium. *J. Coord. Chem.*, **64**(10), 1782-1806.

Sarma, S.J., Tay, J.H., Chu, A. 2017. Finding knowledge gaps in aerobic granulation technology. *Trends Biotechnol.*, **35**(1), 66-78.

Seviour, T., Lambert, L.K., Pijuan, M., Yuan, Z. 2010. Structural determination of a key exopolysaccharide in mixed culture aerobic sludge granules using NMR spectroscopy. *Environ. Sci. Technol.*, **44**(23), 8964-8970.

Shanker, A., Venkateswarlu, B. 2011. Chromium: Environmental Pollution, Health Effects and Mode of Action. *in-Chief: Jerome ON (ed) Encyclopedia of Environmental Health. Elsevier, Burlington*, **65**, 650-659.

Sheng, G.-P., Yu, H.-Q., Li, X.-Y. 2010. Extracellular polymeric substances (EPS) of microbial aggregates in biological wastewater treatment systems: A review. *Biotechnol. Adv.*, **28**(6), 882-894.

Shi, W., Ma, X. 2017. Effects of heavy metal Cd pollution on microbial activities in soil. *Ann. Agric. Environ. Med.*, **24**(4), 722-725.

Singare, P.U., Mishra, R.M., Trivedi, M.P. 2012. Sediment contamination due to toxic heavy metals in Mithi river of Mumbai, *Adv. Anal. Chem.* 2(3), 14-24.

Singha, B., Das, S.K. 2011. Biosorption of Cr (VI) ions from aqueous solutions: Kinetics, equilibrium, thermodynamics and desorption studies. *Colloids Surf. B.*, **84**(1), 221-232.

Sinha, V., Pakshirajan, K., Chaturvedi, R. 2018. Chromium tolerance, bioaccumulation and localization in plants: An overview. *J. Environ. Manage.*, **206**, 715-730.

Snaidr, J., Amann, R., Huber, I., Ludwig, W., Schleifer, K.H. 1997. Phylogenetic

analysis and in situ identification of bacteria in activated sludge. *Appl. Environ. Microbiol.*, **63**(7), 2884-2896.

Sovová, H. 2005. Mathematical model for supercritical fluid extraction of natural products and extraction curve evaluation. *J. Supercrit. Fluids*, **33**(1), 35-52.

Stuermer, D.H., Ng, D.J., Morris, C.J. 1982. Organic contaminants in groundwater near an underground coal gasification site in northeastern Wyoming. *Environ. Sci. Technol.*, **16**(9), 582-7.

Sudha Bai, R., Abraham, T.E. 2003. Studies on chromium (VI) adsorption–desorption using immobilized fungal biomass. *Bioresour. Technol.*, **87**(1), 17-26.

Suja, E., Nancharaiah, Y.V., Krishna Mohan, T.V., Venugopalan, V.P. 2015. Denitrification accelerates granular sludge formation in sequencing batch reactors. *Bioresour. Technol.*, **196**, 28-34.

Sultana, M.-Y., Akratos, C.S., Pavlou, S., Vayenas, D.V. 2014. Chromium removal in constructed wetlands: A review. *Int. Biodeterior. Biodegrad.*, **96**, 181-190.

Sun, F.-y., Yang, C.-y., Li, J.-y., Yang, Y.-j. 2006. Influence of different substrates on the formation and characteristics of aerobic granules in sequencing batch reactors. *J. Environ. Sci. (China)*, **18**, 864-71.

Sun, X.-F., Liu, C., Ma, Y., Wang, S.-G., Gao, B.-Y., Li, X.-M. 2011. Enhanced Cu (II) and Cr (VI) biosorption capacity on poly(ethylenimine) grafted aerobic granular sludge. *Colloids Surf. B.*, **82**(2), 456-462.

Sun, X.-F., Ma, Y., Liu, X.-W., Wang, S.-G., Gao, B.-Y., Li, X.-M. 2010. Sorption and detoxification of chromium(VI) by aerobic granules functionalized with polyethylenimine. *Water Res.*, 44(8), 2517-2524.

Sundaramoorthy, P., Chidambaram, A., Ganesh, K.S., Unnikannan, P., Baskaran, L. 2010. Chromium stress in paddy: (i) nutrient status of paddy under chromium stress; (ii) phytoremediation of chromium by aquatic and terrestrial weeds. *C. R. Biol.*, **333**(8), 597-607.

Talaiekhozani, A., Rezania, S. 2017. Application of photosynthetic bacteria for removal of heavy metals, macro-pollutants and dye from wastewater: A review. *J. Water Process. Eng.*, **19**, 312-321.

Tay, J.H., Liu, Q.S., Liu, Y. 2001. The effects of shear force on the formation, structure and metabolism of aerobic granules. *Appl. Microbiol. Biotechnol.*, **57**(1), 227-233.

Tay, S.T.-L., Moy, B.Y.-P., Jiang, H.-L., Tay, J.-H. 2005. Rapid cultivation of stable aerobic phenol-degrading granules using acetate-fed granules as microbial seed. *J. Biotechnol.*, **115**(4), 387-395.

Wang, J., Li, W.-W., Yue, Z.-B., Yu, H.-Q. 2014a. Cultivation of aerobic granules for polyhydroxybutyrate production from wastewater. *Bioresour. Technol.*, **159**, 442-445.

Wang, L., Liu, X., Lee, D.-J., Tay, J.-H., Zhang, Y., Wan, C.-L., Chen, X.-F. 2018. Recent advances on biosorption by aerobic granular sludge. *J. Hazard. Mater.*, **357**, 253-270.

Wang, R., Peng, Y., Cheng, Z., Ren, N. 2014b. Understanding the role of extracellular polymeric substances in an enhanced biological phosphorus removal granular sludge system. *Bioresour. Technol.*, **169**, 307-312.

Wang, S.-G., Liu, X.-W., Gong, W.-X., Gao, B.-Y., Zhang, D.-H., Yu, H.-Q. 2007. Aerobic granulation with brewery wastewater in a sequencing batch reactor. *Bioresour. Technol.*, **98**, 2142-7.

Wang, Z., Gao, M., She, Z., Jin, C., Zhao, Y., Yang, S., Guo, L., Wang, S. 2015. Effects of hexavalent chromium on performance and microbial community of an aerobic granular sequencing batch reactor. *Environ. Sci. Pollut. Res. Int.*, **22**(6), 4575-86.

Whiteley, A.S., Bailey, M.J. 2000. Bacterial community structure and physiological state within an industrial phenol bioremediation system. *Appl. Environ. Microbiol*, **66**(6), 2400-2407.

Wilén, B.-M., Liébana, R., Persson, F., Modin, O., Hermansson, M. 2018. The mechanisms of granulation of activated sludge in wastewater treatment, its optimization, and impact on effluent quality. *Appl. Microbiol. Biot.*, **102**(12), 5005-5020.

Wilén, B.-M., Onuki, M., Hermansson, M., Lumley, D., Mino, T. 2008. Microbial community structure in activated sludge floc analysed by fluorescence in situ hybridization and its relation to floc stability. *Water Res.*, **42**(8), 2300-2308.

Xu, H., Tay, J.H., Foo, S.K., Yang, S.F., Liu, Y. 2004. Removal of dissolved copper (II) and zinc(II) by aerobic granular sludge. *Water Sci. Technol.*, **50**(9), 155-60.

Yang, S.-F., Tay, J.-H., Liu, Y. 2004. Inhibition of free ammonia to the formation of aerobic granules. *Biochem. Eng. J.*, **17**(1), 41-48.

Yarlagadda, V.N., Joshi, H., Mohan, T.V., Venugopalan, V., Narasimhan, S.V. 2006. Aerobic granular biomass: A novel biomaterial for efficient uranium removal. *Cur. Sci.*, **91**, 503-509.

Zhang, X., Fu, W., Yin, Y., Chen, Z., Qiu, R., Simonnot, M.-O., Wang, X. 2018. Adsorption-reduction removal of Cr (VI) by tobacco petiole pyrolytic biochar: Batch experiment, kinetic and mechanism studies. *Bioresour. Technol.*, **268**, 149-

157.

Zheng, X.Y., Lu, D., Wang, M.Y., Chen, W., Zhou, G., Zhang, Y. 2018. Effect of chromium (VI) on the multiple nitrogen removal pathways and microbial community of aerobic granular sludge. *Environ. Technol.*, **39**(13), 1682-1696.

Zheng, X.-y., Wang, M.-y., Chen, W., Ni, M., Chen, Y., Cao, S.-l. 2016. Effect of Cr (VI) on the microbial activity of aerobic granular sludge. *Desalin. Water Treat.*, **57**(15), 7000-7008.

Zheng, Y.-M., Yu, H.-Q., Liu, S.-J., Liu, X.-Z. 2006. Formation and instability of aerobic granules under high organic loading conditions. *Chemosphere*, **63**(10), 1791-1800.

Zhu, L., Qi, H.-y., Lv, M.-l., Kong, Y., Yu, Y.-w., Xu, X.-y. 2012. Component analysis of extracellular polymeric substances (EPS) during aerobic sludge granulation using FTIR and 3D-EEM technologies. *Bioresour. Technol.*, **124**, 455-459.

Zhu, L., Zhou, J., Yu, H., Xu, X. 2015. Optimization of hydraulic shear parameters and reactor configuration in the aerobic granular sludge process. *Environ. Technol.*, 36(13), 1605-1611.

Zita, A., Hermansson, M. 1997. Determination of bacterial cell surface hydrophobicity of single cells in cultures and in wastewater in situ. *FEMS Microbiol. Lett.*, **152**(2), 299-306.

Acknowledgements

First of all, I would like to express my deepest gratitude to my supervisor, Professor Zhenya Zhang, for providing me the opportunity to pursue a doctorate at the University of Tsukuba. I want to thank him for his valuable guidance, positive attitude and encouraging me to study. His support, encouragement, and trust gave me confidence and courage to complete my doctorate.

I also wish to express my great appreciation to Associate Professor Zhongfang Lei for providing me the opportunity to carry out this research project and for giving valuable guidance, professional knowledge and suggestions for my research and paper during my PhD period. Her meticulous patience and diligent work attitude are worthy of my lifelong learning.

I would like to express my gratitude to Associate Professor Kazuya Shimizu for his valuable advice on my thesis and guidance throughout my research and study.

I would like to express my appreciation to Professor Motoo Utsumi, for his valuable and useful comments on my thesis.

I also would like to thank all the group members in Zhang lab. In the three years of study and life at the University of Tsukuba, all your help and suggestions are very precious.

In addition, special thanks for my motherland, the People's Republic of China, especially to the China Scholarship Council (CSC) for financially supporting me in studying abroad at University of Tsukuba in Japan.

Last, thanks for my parents and friends, without their support, I cannot be who I am now.